Dynamical Stochasticity in Classical and Quantum Mechanics

B. V. CHIRIKOV, F. M. IZRAILEV, D. L. SHEPELYANSKY
Institute of Nuclear Physics, 630090 Novosibirsk, USSR

Contents

In this survey we consider some recent results of investigations of stochastic motion in classical and quantum dynamical systems. We discuss in detail the phenomenon of transient, or temporary stochasticity in quantum mechanics. Results of numerical simulation of this phenomenon are given. Estimates are made of quantum effects in the quasiclassical region. A simple classical model of quantum stochasticity is discussed.

1. *Introduction.*

The term "dynamical stochasticity" in the title of this survey paper emphasizes that we are dealing with a specific case of motion of a completely deterministic (dynamical) system. The fact that the motion in this case turns out to be extremely irregular, complicated and unpredictable, is determined exclusively by the internal dynamics of the system, and is not related to any effect of external random perturbations. This type of dynamical motion has been called *stochastic* or *chaotic*, terms whose vagueness reflects the enormous variety of the different special cases of such motions.

The ever increasing interest in the study of stochastic motion is caused mainly by two factors. First, in various branches of physics, engineering and other sciences, more and more particular problems arise whose solution requires a well developed theory of stochastic motion. Secondly, this unusual (nontrivial) regime of motion builds a bridge between dynamical and statistical laws of physics, which at one time were considered to be contradictory, and gives the possibility of understanding and deriving the latter from the former.

From the view point of applications, stochastic motion is a widespread (and dangerous) instability of nonlinear oscillations, which leads to diffusion in the phase space and to other unpleasant consequences. An example is the loss of charged particles in accelerators [1], plasma traps [2], [3], or in the Earth's radiation belts [4]. Still, sometimes such stochastic instability may also prove to be useful, e.g., for the heating of a plasma by a high-frequency field (cf., for example, [5]) or for realizing stochastic acceleration of charged particles (cf. [6]).

Within the framework of applications of the theory of stochasticity, the problems of main interest are the following:

1. To determine the conditions for stochastic instability of a motion.

2. To find out the statistical properties of stochastic motion, and primarily the rate of diffusion in the phase space of the system. These are the problems that will mainly be discussed in this paper.

In regard to the more fundamental problem of the relation between dynamical and statistical laws of physics, the most "acute" question is: can a strictly deterministic motion (of a dynamical system) be at the same time a random one (in the intuitive sense of the word)? Any detailed discussion of this (partly philosophic) question goes beyond the range of this paper. We would however like to make some brief remarks, since it seems to us important to help overcome the still existing psychological barrier that has been built up by the centuries-long tradition of opposing the deterministic to the random. The development of contemporary ergodic theory, and also the Kolomogorov algorithmic theory of complexity have recently reached such a level that one can give a quite definite answer to the question put above, namely, there exist dynamical (completely deterministic) systems, whose motion is in principle indistinguishable from a "random" motion, whatever the precise meaning that we attribute to

the latter term. The validity of this "global" assertion is related to an interesting feature of the motion of a random dynamical system: in the language of symbolic dynamics, the set of its trajectories is *complete*, i.e., contains all the trajectories. We shall come back to this interesting question later in Sec. 4.2. A systematic and relatively readable (for physicists!) presentation of this circle of questions can be found, for example, in the reviews [7–9]. A fairly realistic example of such random dynamics is the elastic collision of balls in billiards, as was shown in the classic papers of Sinai (cf. [9]). Thus now the example of a truly random process is not the traditional coin, nor the roulette wheel at Monte Carlo, but rather the balls of "Sportloto."

In ergodic theory such systems are termed Bernouilli systems; we shall call them simply random. We recall that such systems can be very simple; in particular, two degrees of freedom are sufficient for random dynamics (cf., for example, [9]).

We shall restrict ourselves to treating Hamiltonian (nondissipative) systems. Such systems are sometimes called conservative, but this term seems to us misleading, since it gives rise to a confusion with the conservation of energy. Actually, the energy of a Hamiltonian system may not be conserved if the Hamiltonian depends explicitly on time. It is however important that even in this case the phase density is conserved (Liouville theorem). This significantly simplifies the statistical analysis of the stochastic motion in Hamiltonian systems, since they possess a simple and well known invariant measure.

Until recently it was supposed that including dissipation simplifies the dynamics, since it seemed that all the trajectories then approach either stable equilibrium or a stable periodic solution (limit cycle), which are the simplest examples of attractors in a dissipative system. We now know that this is not always the case. The first example of a nontrivial (stochastic) attractor was studied in the classic paper of Lorenz [10]. The nontriviality of the Lorenz attractor is related both to the fact that the motion is stochastic and that its geometric structure in the dynamical space of the system is highly singular (Cantor structure). It should be noted that such a structure of a stochastic attractor is typical for so-called Anosov [11] systems with dissipation, which are also Bernouilli systems. One of the types of stochastic attractor was investigated in detail by Smale [12]. So, the recent popularity of the term "strange attractor" is surprising (strange to whom?).

The fundamental difficulty of the theoretical analysis of a motion on a stochastic attractor is related to the fact that one must beforehand find an invariant measure, and it may prove to be highly singular in the original dynamical space. We note, however, that in the case of an Anosov system with a *weak* dissipation one can make approximate use of the simple invariant measure corresponding to the system *without* dissipation, for example, the phase density of a close Hamiltonian system. This follows from the fact that all Anosov systems are structurally stable [11]. But then another difficulty arises, connected with the fact that in many cases of practical interest one has to deal with more general systems, which, in particular, are not structurally stable. For such systems weak dissipation leads, as a rule, to a degeneration of the stochastic motion into a periodic one [13]. True, this degeneration disappears with increasing dissipation, but the invariant measure may then turn out to be quite complicated.

It should be mentioned that a dissipative system is not, strictly speaking, purely dynamical, at least if we are dealing with a real physical system. In fact, the dissipation describes (in a very simplified form) some stochastic process at the molecular level, and is therefore necessarily accompanied by fluctuations, i.e., by some random perturbation external to the dynamical system, which must also generally be taken into account. An excellent review on dissipative stochasticity can be found, for example in [14].

Returning to Hamiltonian systems, we note that in certain simplest cases a complete and rigorous investigation of stochastic motion is possible on the basis of contemporary ergodic theory. It is, for example, the already mentioned Anosov systems. However, such a class of dynamical systems turns out to be rather limited from the application point of view. We mention that recently some advances have been made toward broadening the class of dynamical systems permitting a rigorous mathematical analysis [15].

The main contents of the present survey are some recent results of the physical theory of stochasticity, which is based on models, various approximations and estimates, and supported by numerical simulation. We shall consider both stochasticity in classical mechanics (Sec. 2) and the behavior of quantum systems that are stochastic in the classical limit (Sec. 3). The importance of the latter problem from the physical point of view is that quantum mechanics gives a more exact description of real systems. So the question arises: to what extent the unusual properties of the stochastic motion of a classical system

persist in quantum theory? In principle, the answer to this question has been known for a long time (cf., for example, [43]), although it may appear somewhat unexpected to somebody: the stochasticity is not possible in quantum dynamics at all; more precisely, the time evolution of the wave function (or the density matrix) of a closed quantum system, bounded in phase space, is always almost-periodic, i.e., its frequency spectrum is discrete. In classical mechanics such a motion is regarded as just the opposite of stochasticity, for example, the motion of a completely integrable system.

In the present paper we attempt to resolve this apparent contradiction by using the concept of *transient, or temporal stochasticity*. This approach is based on the introduction of different time scales, so that the different statistical properties of classical dynamics manifest themselves over certain *finite* time intervals of the quantum motion.

If we now apply this approach back to classical mechanics, we arrive at the curious conclusion that here also, an almost-periodic motion, for example, the motion of a completely integrable system, may, under definite conditions, imitate a stochastic process over a finite time interval. This sort of imitation has actually been known for a long time, and moreover is the basic method for studying the statistical properties of macrosystems (in particular, for deriving kinetic equations) in statistical physics. So far as we are aware, such an approach was first taken by Bogolyubov [16], who investigated the statistical properties of a large number $N \to \infty$ of uncoupled linear oscillators, and has completed, in a sense, in paper [25], where the Bernouilli property (randomness) of the classical ideal gas was rigorously proved, also for $N \to \infty$.

A new formulation of the problem, arising naturally in classical mechanics from the analysis of quantum dynamics, is the following: for a fixed (and not necessarily large) number of degrees of freedom of a classical completely integrable system, to find the conditions and the time scales for which imitation of stochastic motion occurs. In particular, such a problem arises in numerical simulation of classical stochasticity. Because of the discrete representation of numbers in a computer, all the trajectories of any dynamical system are then simply periodic. Bearing in mind the wide use of numerical simulation for investigating various dynamical systems, estimates of the accuracy and the limits of such simulation are extremely important. This circle of questions will be discussed in Sec. 4.

We take this opportunity to express our sincere thanks to G. Casati,

J. Ford, J. M. Greene, S. A. Kheifets, J. A. Krommes, Ya. G. Sinai, V. V. Sokolov, J. L. Tennyson, F. Vivaldi, G. M. Zaslavsky for stimulating discussions.

2. *Nontrivial Problems of Classical Hamiltonian Dynamics.*

Nontriviality of a problem is here understood in two senses. On the one hand we have in mind the problems of stochastic motion, which still remains a quite unusual regime of classical dynamics. On the other hand, we refer to those (more complicated) problems which still defy rigorous mathematical analysis. Their solution (partial, of course) is based on a qualitative picture of the mechanism of stochastic motion, approximate estimates and numerical simulation. For Hamiltonian systems the most effective method for such semiempirical investigations is the analysis of nonlinear resonances and their interaction. The corresponding technique is described in detail, for example, in the surveys [17, 18].

In this section we consider several specific problems related to the stochastic behavior of simple systems in classical mechanics.

2.1. *Border of Stochasticity.*

The determination of the border of stochastic instability of nonlinear oscillations is one of the fundamental problems in the theory of stochasticity. Here we must distinguish between the stochasticity border in the space of system parameters, i.e., the critical values of parameters such as the perturbations strength, and the border of stochasticity in the phase space of the system, including the critical value of the energy for a closed system. The latter problem is especially complicated. In fact, the structure of the phase space of nonlinear oscillations is usually characterized by an extremely complex interchange of stable and stochastic components of the motion. An example of such a structure is shown in Fig. 1 and will be discussed in more detail later. That structure has been called a *divided* (into stable and stochastic components) *phase space*.

The complexity of the structure of a divided phase space is determined mainly by two factors. First, this structure is hierarchic, i.e., the interchange of stable and stochastic regions takes place over smaller and smaller spatial scales. Secondly, the border between the stable and stochastic components is itself a stochastic surface. All this makes

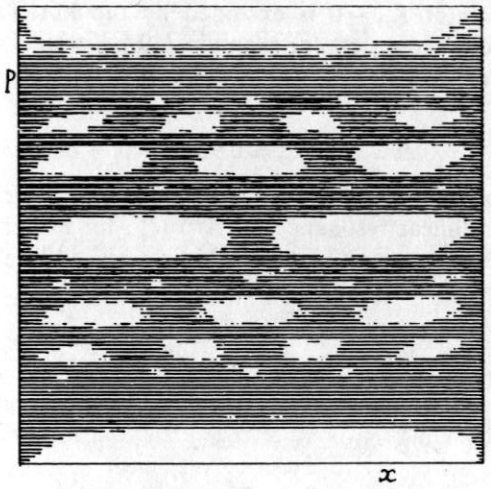

Figure 1. Phase plane of the mapping (2.1.7):

$$a = 0.95; \qquad \sigma = 0.323;$$

$$K = 6.5 \times 10^{-3} > K_{cr} \approx 4.6 \times 10^{-3} \quad \text{(2.1.13)}$$

Stochastic component shaded.

a rigorous analysis of such dynamical systems extremely difficult. Moreover, even the formulation of the problem on the stochasticity border raises some difficulties.

However, there are certain special systems for which one can at least formulate the problem clearly. An example is the so-called standard mapping

$$\begin{aligned} \bar{p} &= p + K \cdot \sin x \\ \bar{x} &= x + \bar{p} = x + p + K \cdot \sin x \end{aligned} \qquad (2.1.1)$$

Many specific problems in the theory of nonlinear oscillations with two degrees of freedom reduce to this mapping (cf., for example, [18]). Here, however, this mapping is of interest to us from a different point of view. The important thing for us is that the phase space of this model (x, p) is periodic not only in x, but also in p (with period 2π). Thus there exists a critical value of the single parameter of this mapping $K = K_{cr}$, above which the motion becomes unbounded.*

*For $K > K_{cr}$ the motion is stochastic [18]. Actually, even for $K < K_{cr}$ there are stochastic regions of complex structure bounded in p. Therefore the condition $K = K_{cr}$ should be understood as the border of global, or connected, stochasticity.

The trivial case of $K_{cr} = 0$ is excluded by the KAM theory (Kolmogorov-Arnold-Moser. cf., for example, [19]).

Numerical experiments with the standard mapping gave the result [18]:

$$K_{cr} \approx 0.989 \tag{2.1.2}$$

In order of magnitude this result could be gotten from a simple criterion of nonlinear resonance overlap (cf., for example, [18]). For this purpose the mapping (2.1.1) should be replaced by the equivalent continuous system with the Hamiltonian

$$H(x, p, t) = \frac{p^2}{2} + K \sum_{n=-\infty}^{\infty} \cos(\theta - 2\pi n t) \tag{2.1.3}$$

If we take account only of the resonances in first approximation $\dot{\theta} \approx p = 2\pi n$, we have

$$K_{cr}^{(1)} = \frac{\pi^2}{4} \approx 2.5 \tag{2.1.4}$$

More complicated calculations involving resonances of higher approximations, and also the stochastic layer of resonances, enable one [18] to improve the agreement with the numerical result (2.1.2): $K_{cr} \approx 1.1$.

An entirely different approach to the solution of the problem on the stochasticity border was recently developed by Greene [20]. His approach is based on the study of trajectory stability at the center of resonances. Generally, this method always overestimates K_{cr}, since the unbounded motion is possible over a set of touching (intersecting) separatrices, while the resonance centers are still stable. Thus, for example, the fixed points of the mapping (2.1.1) $x = \pi$; $p = 2\pi n$, i.e. the trajectories with period $T = 1$ at the resonance centers, remain stable up to $K = K_1 = 4$, which exceeds even the value (2.1.4). However, already $K_2 = 2$ ($T = 2$); $K_3 = 1.52$; $K_4 = 1.24$ etc. [21]. Thus Greene's hypothesis that, as $T \to \infty$, $K_T \to K_{cr}$ seems to be plausible. His result for the standard mapping [20]:

$$K_{cr} = 0.971635\ldots \tag{2.1.5}$$

is noticeably less than the value (2.1.2). In connection with this discrepancy, we have carried out a new, more careful processing of the numerical data given in [18]. But the new result $K_{cr} \approx 1.00$ increased the discrepancy even more.

One of the reasons for this discrepancy may be the following. The investigation of the stability of periodic trajectories for large T can be

carried out only numerically. One can therefore not run through all the periodic trajectories, and so one has to assume the additional hypothesis that the most stable periodic trajectories at resonance centers are those with the unperturbed ($K = 0$) frequency

$$\frac{\omega}{2\pi} = \frac{M}{T} \to g = \frac{1}{1 + \dfrac{1}{1 + \cdots}} = \frac{\sqrt{5} - 1}{2} \approx 0.618 \tag{2.1.6}$$

where M, T are integers, T being the full period of the trajectory before it closes. Greene calls the number g "the most irrational number" on the grounds that it is the most poorly approximated by rationals, as one sees from the representation of g by a continued fraction (2.1.6). From the viewpoint of resonance overlap, however, this last hypothesis of Greene does not seem convincing, since for the overlap not only the spacing between resonances but also their width, which depends on the denominator of the rational $\omega/2\pi = M/T$, is of importance.

For a more detailed investigation of this question we chose a somewhat different model, given by the mapping [22]:

$$\bar{p} = p + \frac{K \cdot \sin x}{(1 - a \cdot \cos x)^2}$$
$$\bar{x} = x + \bar{p} \tag{2.1.7}$$

Unlike the standard mapping, the perturbation in this system already contains many harmonics in phase x in first approximation (for $a \to 1$):

$$\frac{\sin x}{(1 - a \cdot \cos x)^2} \approx \frac{2}{\sigma} \sum_{m=1}^{\infty} e^{-\sigma m} \cdot \cos mx \tag{2.1.8}$$

where $\sigma \approx \sqrt{1 - a^2}$. Thus, already in the first approximation there "operate" not only integer resonances $p = 2\pi n$, but also fractional ones, $p = 2\pi n/m$ (with $m \lesssim 1/\sigma$), as one sees from the Hamiltonian of the equivalent continuous system [22]:

$$H(x, p, t) \approx \frac{p^2}{2} + \frac{2K}{\sigma} \sum_{m=1}^{\infty} e^{-\sigma m} \sum_{n=-\infty}^{\infty} \cos(mx - 2\pi n t) \tag{2.1.9}$$

First, let us consider each of the resonances individually in the "pendulum" approximation [18]. The halfwidth of the resonance

separatrix is equal to

$$(\Delta p)_m = 2\sqrt{\frac{2K}{\sigma}}\, e^{-\sigma m/2} \tag{2.1.10}$$

while the simple sum over all resonances in the interval $0 \leqslant \omega/2\pi \leqslant 1$ is

$$S(K,\sigma) = 2\sum_{m=1}^{\infty}\sum_{n=1}^{m}(\Delta p)_m = 4\sqrt{\frac{2K}{\sigma}}\sum_{m=1}^{\infty} m e^{-\sigma m/2}. \tag{2.1.11}$$

From the condition $S(K,\sigma) \approx 2\pi$ one can obtain a rough estimate of K_{cr} in the form

$$K_{cr} \approx \frac{\pi^2}{128}\sigma^5 \tag{2.1.12}$$

This estimate can be improved as follows [22]. We should take the sum in (2.1.11) not over all m, n, but only over those m_0, n_0 that form irreducible fractions n_0/m_0. The number of these irreducible resonances is on the average $2/3$ of all the resonances. The remaining resonances split up into groups, each corresponding to one irreducible resonance: $m = m_0 l$; $n = n_0 l$, $l = 1, 2, \ldots$. For $\sigma \ll 1$, the motion in the neighborhood of each irreducible resonance is determined by all the perturbation terms in the Hamiltonian (2.1.9) belonging to this group, i.e., by the sum over l for given m_0, n_0. As a result, the pendulum approximation is violated, and the resonance width for low harmonics ($\sigma m_0 \lesssim 1$) increases significantly.

However, it is most important to take account of nonuniformity in resonance spacing. In fact, the total number of resonances with $m_0 \leqslant m_1$, per unit interval of the quantity $\omega/2\pi$, is $(2/3)m_0^2$, so that the average spacing between resonances is $\langle \Delta\omega \rangle \approx 3\pi/m_0^2$. But near the integer resonances (for example, $n_0/m_0 = 1$) the gaps are formed equal to $(\Delta\omega)_1 = 2\pi/m_0$. So it is clear that K_{cr} is actually determined not by the average overlap of resonances (2.1.11), but by the "covering" of these gaps. This significantly increases the critical perturbation for this model [22]:

$$K_{cr} \approx \frac{\pi^2\sigma^4}{(L + 4/L)^2}; \qquad L = \ln\frac{128}{9\sigma} \tag{2.1.13}$$

Some results of a numerical simulation of the system (2.1.7) were described in [23]. The simulation was done as follows. Suppose that

we are interested in the dynamics of the system

$$\begin{aligned} \bar{p} &= p + K \cdot f(x) \\ \bar{x} &= x + \bar{p} \end{aligned} \tag{2.1.14}$$

where $f(x)$ is a periodic function of period 2π. We consider the auxiliary mapping

$$\begin{aligned} \bar{y} &= y + \frac{f(x)}{\lambda} \\ \bar{x} &= x + \lambda \cdot F(\bar{y}) \end{aligned} \tag{2.1.15}$$

where λ is some constant; $f(x)$ is the same function as in (2.1.14), while $F(y)$ is a new function that we will choose later.

We linearize the second equation of this last mapping around one of the resonant values $y = y_{cr}$, where

$$\lambda \cdot F(y_r) = 2\pi r; \qquad r = \text{integer}. \tag{2.1.16}$$

Setting $p = \lambda \cdot F'(y_r)(y - y_r)$, we get back the original mapping (2.1.14) with the parameter

$$K = F'(y_r) \tag{2.1.17}$$

Now suppose that the function $|F'(y)|$ falls off monotonically with $|y|$; then the condition $|K| > K_{cr}$ determines the stochastic layer $|y| < v_b$ on the phase plane of the auxiliary mapping (2.1.15). Also, conversely, if by computation we find the maximum value $y_m \approx y_b$ ($|y| < y_m$) which diffusion in the system (2.1.15) reaches, then from (2.1.17) we can approximately estimate the critical perturbation for the mapping (2.1.14): $K_{cr} \approx |F'(y_m)|$. More precisely, we can assert that

$$K_{cr} \leqslant |F'(y_l)| \tag{2.1.18}$$

where y_l corresponds to the last integer resonance crossed by the trajectory ($\lambda F(y_l) = 2\pi r$). If the original mapping (2.1.14) is symmetrical in respect to $p = \pi$, i.e., in respect to the half-integral resonance, as is the case, for example, in the standard mapping ($f(x) = \sin x$), and also in the mapping (2.1.7) under consideration, then y_l in (2.1.18) corresponds to the last half-integer resonance ($\lambda \cdot F(y_l) = \pi r$).

As the auxiliary function we chose $F(y) = \ln|y|$. We note that for $f(x) = \sin x$ the mapping (2.1.15) describes the motion in the stochastic layer of the nonlinear resonance in the pendulum approximation

[18]. Numerical experiments with the mapping (2.1.15) and $f(x)$ from (2.1.7), for a number of iterations $t \sim 10^6$, showed a good agreement of K_{cr}, determined by this method, with the estimate (2.1.13) in the range $0.03 < \sigma < 0.5$ [23]. However, as the motion time increases further, the critical value K_{cr} slowly "creeps" downward. Thus, for $\sigma = 0.142$ and $t = 2 \times 10^8$, the upper limit of K_{cr} (2.1.18) dropped to 4.3×10^{-5}, whereas the estimate (2.1.13) gives 1.3×10^{-4}. The fact that this last value, obtained from the overlap of the first approximation resonances, is too high, would be rather natural (cf. the critical value (2.1.4) for the standard mapping). The interesting point is another one, in that the ratio R of the theoretical and numerical values of K_{cr} ($R \approx 3$) differs only slightly from the corresponding ratio for the standard mapping ($R \approx 2.5$, cf. (2.1.4)). We may add that in the case of just two overlapping resonances, $R \approx 2.3$ (from the data of [18]) and $R \approx 2$ (from the data of [24]).

In the case considered here this ratio can be interpreted differently, as a reduction in the effective value $\sigma \to \sigma^*$ due to the effects of higher approximations. From the value $R \approx 3$ above and the estimate (2.1.13) we have $\sigma^*/\sigma \approx 0.76$.

An indirect confirmation of the decisive role of the gaps near the integer resonances, on which (2.1.13) is based, is the histogram in Fig. 2. Here the fractional part $r = \{\lambda F(y_m)/2\pi\}$ characterizes the location of the system within the period of the resonance structure corresponding to the maximum value $|y| = y_m$ reached at the given time. The ordinate gives the number of iterations T during which y_m remained within each of 20 intervals covering a period of the resonance structure. The horizontal arrow in the upper part of the Figure shows the direction of diffusion. It is clear that the most difficult section to get through is that immediately before the integer resonance $r = 1$. The two vertical arrows show the "most irrational" (à la Greene) values $r = g$ (2.1.6) and $r = 1 - g$, in the neighborhood of which no significant delay of the diffusion is observed.

Although the agreement obtained between the last computational results and the estimate (2.1.13), based on the relatively simple overlap criterion appears satisfactory, this question requires further study, in particular the performance of further numerical experiments over a much longer time of the motion. The latter is connected with a very slow diffusion in the region of a gap. This may lead to a further reduction in the numerical value of K_{cr}. In addition it is not excluded that the quite high accuracy of numerical compuation (56 binary

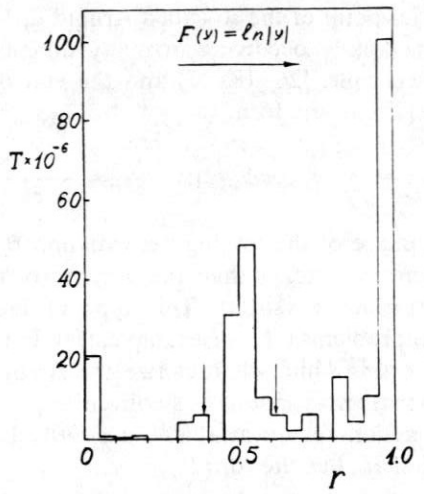

Figure 2. Histogram of "passability" for various sections of the resonance set: $r = \{\lambda F(ym)/2\pi\}$, T is the sojourn time (number of iterations) of y_m in the given interval of the period of the resonance structure.

digits in the mantissa) may still be insufficient, again because of the low diffusion rate. Then, "cycling" may occur, i.e., the change to a periodic trajectory because of the discrete representation of numbers in the computer (cf. Sec. 4.2).

2.2. *The Modulation Diffusion.*

As mentioned earlier, the structure of the stochastic components in phase space is usually very complicated. In this section we consider a fairly simple and little-known case, where the stochastic components have the form of relatively narrow layers, along which the system can diffuse over considerable distances. Such a structure arises, for example, as a result of weak low-frequency modulation in the system.

Let us consider the case of external modulation. As an example, we take a system with the Hamiltonian

$$H = \frac{p_1^2 + p_2^2}{2} + \frac{x_1^4 + x_2^4}{4} - \mu x_i x_2 - \epsilon x_i f(t) \qquad (2.2.1)$$

This Hamiltonian describes the behavior of two coupled nonlinear oscillators driven by the force $f(t)$. The system (2.2.1) was studied

earlier from the viewpoint of the so-called Arnold diffusion which is a weak universal instability occurring in many dimensional oscillator systems (cf., for example, [26, 18, 27] and the end of Sec. 2.3). We choose $f(t)$, as in [27], in the form

$$f(t) = \sum_{m=1}^{\infty} f_m \cos\psi_m(t); \qquad f_m = \frac{2e^{-\sigma m}}{\sigma} \tag{2.2.2}$$

Suppose that the phase of the driving perturbation $f(t)$ is modulated at a frequency Ω much smaller than the unperturbed frequencies of the system: $\psi_m(t) = m\nu t + \lambda \sin \Omega t$. This type of modulation often occurs in practical problems (cf., for example, [1]). For small values of the parameters $\mu, \epsilon \ll 1$, which characterize the strengths of the coupling and the driving perturbation, it is convenient to change to I_i, θ_i, the unperturbed action-angle variables ($\mu, \epsilon = 0$). Then the unperturbed Hamiltonian H_0 has the form:

$$H_0 = C_0(I_1^{4/3} + I_2^{4/3}); \qquad C_0 \approx 0.87 \tag{2.2.3}$$

In this approximation the actions I_1 and I_2 are constants, while we have for the phase angles θ_1 and θ_2:

$$\dot{\theta}_1 = \omega_1(I_1); \qquad \theta_2 = \omega_2(I_2) \tag{2.2.4}$$

where ω_1, ω_2 are the unperturbed frequencies of the system, depending on I_1, I_2 because of the nonlinearity of the oscillations. Despite the strong nonlinearity, the oscillations are close to harmonic: $x_i(t) \approx a_i \cos\theta_i(t)$, while their frequencies are proportional to the amplitudes: $\omega_i \approx 0.85 a_i$.

The parameter λ in (2.2.4) determines the modulation factor. In the absence of modulation the system has driving resonances $\omega_1(I) = m\nu$ and a coupling resonance $\omega_1(I_1) = \omega_2(I_2)$ (cf. Fig. 3). If the perturbation is large enough, neighboring nonlinear resonances overlap, and strong stochasticity appears, leading to a rapid rise of the total energy.

Here we would like to call attention to the possibility of the so-called modulation diffusion [28] which is similar in a certain sense to the Arnold diffusion. The cause for the appearance of this diffusion in the case of $\lambda \neq 0$ is the overlap of modulation resonances around each of the driving resonances.

Let us find the condition for overlap of modulation resonances near a single driving resonance of harmonic m. To do this we write the

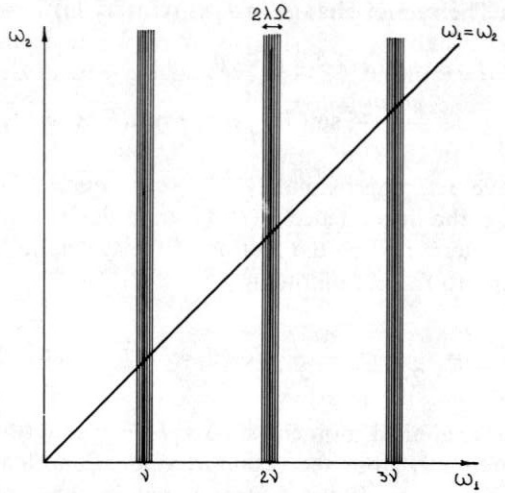

Figure 3. Pattern of the first approximation resonances for the system (2.2.1): ω_1, ω_2 are the oscillator frequencies; ν is the mean frequency of the driving force; Ω is the frequency of the modulation causing the formation of the multiplets.

Hamiltonian of the motion in x_1 without coupling ($\mu = 0$) and near a particular modulation resonance ($\omega_1 = m\nu + n\Omega$):

$$H_M = C_0 I_1^{4/3} - \frac{\epsilon}{2} f_m a_1(I_1) \mathcal{J}_n(\lambda) \cos(\theta_1 - m\nu t - n\Omega t) \tag{2.2.5}$$

where $\mathcal{J}_n(\lambda)$ is a Bessel function. Estimating the resonance width $\Delta\omega_1$ and comparing it with the spacing between resonances Ω we obtain the resonance overlap parameter:

$$s = \frac{\Delta\omega_1}{\Omega} \sim \frac{4\omega_1 e^{-\sigma m/2}}{a_1^{3/2}\Omega\sqrt{\sigma}} \cdot \left(\frac{\epsilon^2}{\pi\lambda}\right)^{1/4} \tag{2.2.6}$$

where we have used the estimate $\mathcal{J}_n(\lambda) \sim 1/\sqrt{\pi\lambda}$ for $\lambda \gg 1$. For $K_m \approx 2.5 s^2 > 1$, [18], a modulation stochastic layer is formed with width $\approx 2\lambda\Omega$. We have here introduced a stability parameter K_M, analogous to the parameter K of the standard mapping (2.1.1).

Let us take $\lambda\Omega \ll \nu$, so that neighboring modulation layers do not touch each other (cf. Fig. 3), and any significant diffusion is possible only along the layer, with increase in the energy of the other degree of

freedom (I_2). The rate of change in I_2 is (cf. (2.2.1)):

$$\dot{I}_2 \approx -\mu a_1 \cos\theta_1 \cdot a_2 \sin\theta_2$$
$$\approx \frac{\mu a_1 a_2}{2}\left[\sin(\theta_1 - \omega_2 t) - \sin(\theta_1 + \omega_2 t)\right] \qquad (2.2.7)$$

where we have set, approximately, $\theta_2 \approx \omega_2 t$. For sufficiently small coupling $\mu \ll \epsilon$, the dependence $\theta_1(t)$ differs little from the case when $\mu = 0$, and is determined by the motion of the system in the stochastic layer according to the Hamiltonian:

$$H_{x_1} = \frac{\omega_1^2 \Delta^2}{2a_1^4} = \frac{\epsilon a_1 f_m}{2} \cos(\theta_1 - m\nu t - \lambda \sin \Omega t) \qquad (2.2.8)$$

Here the new canonical momentum $\Delta = I_1 - I_r$ describes the deviation of the action I_1 from the resonant value I_r, which satisfies the condition: $\omega_1(I_r) = m\nu$. If the system is within the modulation stochastic layer, the change in I_2, according to (2.2.7), is of diffusion nature and is determined by the correlation properties of the phase $\theta_1(t)$. The rate of this diffusion will be found in the next Section.

We note that the diffusion mechanism in I_2 can be regarded as a "pumping over of the stochasticity" from one degree of freedom to the other. Such a picture of the diffusion in the stochastic layer was proposed in [29], where a similar problem was considered. Actually, a similar mechanism for the "transfer" of stochasticity had been discussed briefly still earlier in [30].

2.3. *Statistical Properties of Stochastic Motion.*

For the solution of concrete problems related to stochastic motion of dynamical systems, in addition to the border of stochasticity or, in the more general case, the (geometrical) structure of the stochastic component, one must know the statistical properties of the motion in the stochastic region. The most important of these is the diffusion rate in the stochastic component. In some cases this problem is trivial. Thus, for example, for the standard mapping (2.1.1), with $K \gg 1$, i.e., sufficiently deep within the stochastic region, the successive values of the phase x can be regarded to a good accuracy as random and independent [18]. It then immediately follows that the rate of diffusion in p is:

$$D_p \equiv \frac{\langle(\Delta p)^2\rangle}{t} \approx \frac{K^2}{2} \qquad (2.3.1)$$

which agrees well with the results of numerical simulation [18].

But the situation is not always so simple. For example, in the problem of modulation diffusion (Sec. 2.2) the rate of diffusion is determined by the square of the Fourier component modulus of a certain random continuous function (2.2.7). This means that, in the general case, we must know the Fourier spectrum of the random process, or the associated correlation function of the motion. Either of these, of course, depends on the structure of the stochastic component. For the problem of modulation diffusion the latter arises because of the overlap of several "parallel" resonances (Fig. 3).

To study the statistical properties of such a component we consider the following simple model with the Hamiltonian:

$$H(x, p, t) = \frac{p^2}{2} + k \cdot \cos(x + \lambda \cdot \cos \Omega t) \qquad (2.3.2)$$

Here Ω is the modulation frequency, while λ determines the modulation factor (the effective number of lines in the multiplet); the total width of the modulation spectrum is known to be approximately $2\lambda\Omega$. The condition for formation of a stochastic layer is (cf. Sec. 2.2):

$$K_M \approx 2.5 s^2 \sim 23 \cdot \frac{k}{\sqrt{\lambda}\,\Omega^2} > 1 \qquad (2.3.3)$$

where s is the overlap parameter for the modulation resonances. We shall assume that this condition is well satisfied, so that a quite uniform stochastic layer is formed. Then the dynamics of the system (2.3.2) is described by some random function $x(t)$ and we must find its correlation properties.

We introduce the auxiliary dynamical variable z, whose change is determined by the equation:

$$\dot{z} = \epsilon \cdot \sin(qx - \omega t) \qquad (2.3.4)$$

where ϵ, q, ω are constants. This equation has the same form as (2.2.7) (with $q = 1$) in the problem of modulation diffusion. Thus the latter corresponds to diffusion in z for the model under consideration. We have slightly generalized the model (2.3.2,4) by introducing a new

parameter q which is relevant in the other cases of modulation diffusion.

We can first draw some preliminary qualitative conclusions about the dependence of the diffusion rate

$$D \equiv \frac{\overline{(\Delta z)_t^2}}{t}\,; \qquad (\Delta z)_t = \epsilon \int_0^t \sin(qx(t') - \omega t')\,dt' \qquad (2.3.5)$$

on the perturbation frequency ω. In the interval $|\omega| \lesssim q\lambda\Omega$ the rate of diffusion is approximately constant and relatively high since within this interval the exact resonance $qx = \omega$ does occur (cf. (2.3.5)) due to the diffusion in frequency $\dot{x} = p$ which fills up all the modulation stochastic layer $|p| \lesssim \lambda\Omega$. On the other hand, for $|\omega| \gg q\lambda\Omega$ the diffusion rate falls off exponentially since the function $\sin(qx(t))$ is analytic (cf. (2.3.2)), and the Fourier spectrum of any analytic function is known to be exponential as $|\omega| \to \infty$. Let

$$D \to A \cdot \exp\left(-\frac{|\omega|}{\omega_1}\right); \qquad \omega \gg \omega_1 \qquad (2.3.6)$$

The most important problem is the determination of the scale of exponential falloff ω_1. Since we don't know any analytic method for solution of this problem, we went over to a numerical simulation of the combined system (2.3.2), (2.3.4).

When $k \ll 1$ the differential equations of motion can be replaced approximately by the mapping:

$$\begin{aligned} \bar{p} &= p + k \cdot \sin(x + \lambda \cdot \cos \Omega t) \\ \bar{x} &= x + \bar{p} \\ \bar{z} &= z + \epsilon \cdot \sin(qx - \omega t) \end{aligned} \qquad (2.3.7)$$

where t now takes on only integer values and $|\omega| \ll 2\pi$. To reduce the "background" associated with the discreteness of this computational scheme, we used an averaging of $z(t)$ over the ten intervals into which the total time of computation was divided. This very efficient technique is described at length in [26, 18].

We first consider the case of $q = 1$. Preliminary numerical experiments showed that the exponent scale is approximately proportional to the width of the stochastic layer. Figure 4 gives the dependence of $D(\omega)$ in normalized coordinates: $\log(D_R)$, $y = \omega/\Delta\omega$, where $D_R = \Delta\omega \cdot D/\epsilon^2$ is the renormalized diffusion rate, and $\Delta\omega$ is the actual halfwidth of the layer, which usually somewhat exceeds $\lambda\Omega$. In the Figure are collected data for various values of the model parameters

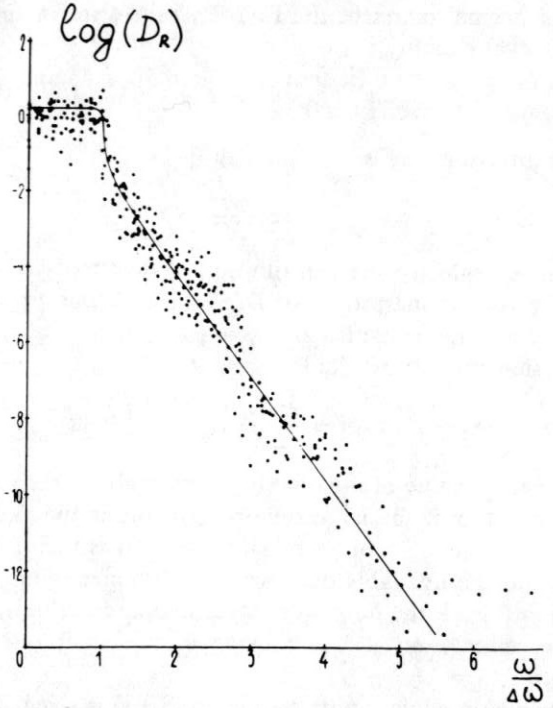

Figure 4. Frequency dependence of the rate of modulation diffusion (for the notation, see the text; logs are base 10). The points are numerical values of the diffusion rate in z for the system (2.3.2), (2.3.4) with $q = 1$. The solid curve is drawn from formula (2.3.18) with the average empirical values $\langle\alpha\rangle = 6.21$, $\langle\beta\rangle = \pi - 0.065$.

in the intervals:

$$\begin{aligned} &10^{-5} \leqslant k \leqslant 3 \times 10^{-3}; \qquad 0.014 \leqslant \Delta\omega \leqslant 0.36 \\ &10^{-3} \leqslant \Omega \leqslant 2 \times 10^{-2}; \qquad 3.8 \leqslant s \leqslant 30 \\ &10 \leqslant \lambda \leqslant 100 \end{aligned}$$

Disregarding the quite large fluctuations, we note the following features of the function $D(\omega)$:

1. a plateau $|\omega| \lesssim \Delta\omega$ with maximum diffusion rate;
2. an exponential "tail" for $\omega > \Delta\omega$ with $\omega_1 = \Delta\omega/\alpha$, where the average value of α for all the data is $\langle\alpha\rangle = 6.21 \pm 0.17 \approx 2\pi$;
3. a sharp drop in the diffusion rate at $|\omega| \approx \Delta\omega$;
4. an irregular dependence of $D(\omega)$ on the "tail."

The maximum diffusion rate on the plateau can be found from the

condition of normalization of the Fourier transform for the function $\sin x(t)$ (Parseval equality):

$$\int_{-\infty}^{\infty} D_R(y)\,dy = \pi \tag{2.3.8}$$

whence the diffusion rate on the plateau ($|\omega| < \Delta\omega$) is:

$$D^{(\mathrm{pl})} \approx \frac{\pi\epsilon^2}{2\lambda\Omega} \tag{2.3.9}$$

where we have neglected the contribution of the "tail" to the integral (2.3.8) in view of the sharp drop of $D(\omega)$ for $|\omega| > \Delta\omega$. From the data in Fig. 4, the average value is $\langle D_R^{(\mathrm{pl})} \rangle = 1.21 \pm 0.10$.

The diffusion rate on the "tail" is

$$D_R \approx B \cdot \exp\left(-\frac{2\pi|\omega|}{\Delta\omega}\right); \qquad |\omega| > \Delta\omega \tag{2.3.10}$$

where the average value of the quantity B over all the data of Fig. 4 is $\langle B \rangle = 16$. Because of the large fluctuations, the individual values of B differ by more than an order of magnitude. It is therefore difficult to decide from the available data whether B depends on the system parameters, although the numerical results apparently indicate such a dependence, mainly on the parameter λ. We shall return to this question later.

The frequency modulation in the model (2.3.2) is a regular external perturbation, and the question arises to what extent the empirical diffusion rate that we have found depends on this regularity. To clarify this question the frequency modulation was replaced by a "random" perturbation in the form of a set of harmonics with random phases. The results of these numerical experiments show that the exponent scale then changed insignificantly ($\langle \alpha \rangle = 5.74 \pm 0.15$), while the value of B decreased substantially ($\langle B \rangle = 3.4$). Such a change in B apparently provides additional indirect evidence for a dependence of that quantity on the model parameters.

However, the regularity of the frequency modulation manifests itself in a different way—in a dependence on the system parameters of the so-called KS-entropy h (the Krylov-Kolmogorov-Sinai entropy), which determines the average rate of exponential divergence for close trajectories of the system. Namely, it turned out that the numerical values of h are very well described by the simple relation

$$h = \frac{\Omega}{2\pi} \ln \frac{K_M}{2} \approx \frac{\Omega}{\pi} \ln s \tag{2.3.11}$$

where K_M is given by (2.3.3). This relation coincides exactly with the expression for the KS-entropy of the standard mapping (upon the replacement of K by K_M, cf., for example [18]).

This coincidence becomes understandable if we transform the mapping (2.3.7) for our model. Let us introduce a new phase $u = x + \lambda \cos \Omega t$, then the first of the two equations in (2.3.7) may be rewritten in the form ($\Omega \ll 2\pi$):

$$\begin{aligned} \bar{p} &= p + k \cdot \sin u \\ \bar{u} &\approx u + \bar{p} - \lambda\Omega \cdot \sin \Omega t \end{aligned} \tag{2.3.12}$$

This mapping models the periodic crossing the resonance $p = \lambda\Omega \sin \Omega t$, and that process can actually be described using the standard mapping, at least in a certain range of the parameters [31].

For sufficiently slow resonance crossing ($\Omega^2 \ll k/\lambda$), within the modulation stochastic layer there is a stable domain, but not a fixed one, as for example in Fig. 1, but rather an oscillating domain. In particular, its center moves according to the law:

$$p_0 \approx \lambda\Omega \cdot \sin \Omega t; \qquad x_0 \approx \pi - \lambda \cdot \cos \Omega t \tag{2.3.13}$$

We found such a stable region, indeed. It should be noted that its relative phase area, which is readily obtained from (2.3.12),

$$\sigma \approx \frac{4\sqrt{k}}{\pi\lambda\Omega} \approx \frac{s}{\pi\lambda^{3/4}} \tag{2.3.14}$$

is usually small ($s \ll \lambda$), so that, for most initial conditions within the modulation layer, the motion is stochastic.

We note that the phenomenon of slow resonance crossing gives an interesting example of a process for which overlapping of resonances can, under certain initial conditions, lead to a regular rather than stochastic motion.

For a "random" perturbation the expression (2.3.11) no longer works. Instead, a "typical" estimate for h, obtained in [31] on the basis of the notion of renormalized resonances, holds approximately

$$h_T \approx 0.066\Omega s^{4/3} \tag{2.3.15}$$

The numerical factor in this expression is taken from [32], where it was obtained by solving the corresponding kinetic equation in the quasilinear approximation. The average ratio of the computed values of h to the theoretical values (2.3.15) is $\langle h/h_T \rangle = 0.89 \pm 0.05$.

Renormalization of resonances is carried out as follows [31]. The

renormalized resonance width ($\Delta\omega'$) is determined by all the perturbation harmonics that fall within the renormalized width, where, because of the randomness of different harmonic phases, the squared amplitudes, i.e., the fourth powers of the nonrenormalized widths of the individual resonances ($\Delta\omega$), are summed up. Then

$$(\Delta\omega')^4 \sim (\Delta\omega)^4 \frac{(\Delta\omega')}{\Omega}$$

and

$$h \sim \Delta\omega' \sim \frac{(\Delta\omega)^{4/3}}{\Omega^{1/3}} \sim \Omega \cdot s^{4/3}$$

since $s \sim (\Delta\omega/\Omega)$.

The KS-entropy also may be considered as one of the important statistical properties of stochastic motion. Although it is not directly related to the diffusion rate, as is clear from the examples just considered, the local instability of motion, which it characterizes, is a decisive mechanism for the appearance of statistical properties of the dynamical motion. On the other hand, it is interesting to note that there is the inverse dependence as well: the random perturbation (with continuous spectrum) depending on coordinates does always result in an exponential local instability of the motion, as directly follows from the derivation of the relation (2.3.15) in [32].

A general description of the correlation spectrum $D_R(y)$ can be given on the basis of the following notions. We shall assume that the spectrum is determined by two different mechanisms:

1. a local law of stochastic motion with spectrum $d_R(y)$;
2. a shift of this spectrum by an amount $q \cdot p$ because of diffusion across the stochastic layer.

The resulting spectrum is then determined by the convolution

$$D_R(y) = \frac{1}{2q} \int_{-q}^{q} d_R(y - y_1)\, dy_1 \tag{2.3.16}$$

The local spectrum can be fitted using the relation

$$d_R(y) = \frac{\pi}{2} d \frac{\sin\beta}{\beta} \cdot \frac{1}{\cos\beta + \cosh(\alpha y)} \tag{2.3.17}$$

where β is an additional parameter, related to the quantity B in (2.3.10). Then the total spectrum, including the plateau, the drop and the exponential "tail," may be described by

$$D_R(y) = \frac{\pi}{2q\beta}\left[\arctan\left(\tanh\left(\alpha\frac{q-y}{2}\right)\tan\frac{\beta}{2}\right) + \arctan\left(\tanh\left(\alpha\frac{q+y}{2}\right)\tan\frac{\beta}{2}\right)\right] \tag{2.3.18}$$

Performing the Fourier transform, we get the correlation function of the process $\sin x(t)$ in the form

$$R(\tau) = \frac{\pi}{\beta}\frac{\sin(q\Delta\omega\cdot\tau)}{q\Delta\omega\cdot\tau} \cdot \frac{\sinh\left(\frac{\beta\Delta\omega\cdot\tau}{\alpha}\right)}{\sinh\left(\frac{\pi\Delta\omega\cdot\tau}{\alpha}\right)} \to e^{-\xi\Delta\omega\cdot\tau/\alpha} \qquad \tau\to\infty \tag{2.3.19}$$

where $\xi = \pi - \beta$. Thus asymptotically as $\tau \to \infty$ the correlation decays exponentially, although initially, when the correlation is still large, it decays only as $1/\tau$.

It follows from (2.3.19) that the exponent is determined by two dimensionless parameters ξ, α. Since α is a constant ($\alpha \approx 2\pi$) the dependence on the system parameters is determined by ξ alone, which is related to the drop of the spectrum, or to the parameter B:

$$B = \tau \frac{\sin\xi}{\pi - \xi} \cdot \frac{\sinh(\alpha q)}{q} \tag{2.3.20}$$

One may assume that the rate of exponential decay of correlations in (2.3.19) is proportional to the KS-entropy h:

$$R(\tau) \sim \exp(-C \cdot h\tau); \qquad \tau\to\infty \tag{2.3.21}$$

where C is some constant independent of the system parameters. We then obtain a relation between ξ, h, C:

$$\xi = C\frac{\alpha h}{\Delta\omega} \tag{2.3.22}$$

For modulation diffusion,

$$\xi = 2C\frac{\ln s}{\lambda} \tag{2.2.23}$$

Our numerical experiments give the following average value for the constant: $C = 0.47 \pm 0.21$. The large error is related to big fluctuations (cf. Fig. 4).

For the "random" perturbation the expression for ξ takes the form:

$$\xi \approx 0.13 C \frac{s^{4/3}}{\lambda} \tag{2.3.24}$$

The average measured value is $C = 0.13 \pm 0.028$.

For $q \neq 1$ the correlation spectrum $D(\omega)$ suffers the following changes:

1. as expected, the size of the plateau becomes equal to $q\Delta\omega$ (for $q > \xi/\alpha$), and the diffusion rate on the plateau is $D(\omega) \approx (\pi\epsilon^2/2q\lambda\Omega)$.

2. in the exponential dependence on the "tail" only the coefficient B changes (cf. (2.3.20)).

These changes are well described by the relations (2.3.16–18). Thus, for $q < \xi/\alpha$ the size of the plateau is independent of q, in agreement with (2.3.18).

For the diffusion rate on the "tail" we finally get ($\xi \ll 1$, $q > 1/2\pi$):

$$D(w) \approx \frac{\epsilon^2 \ln s}{2\lambda^2 \Omega q} \cdot \exp\left(-2\pi\left(\frac{\omega}{\Delta\omega} - q\right)\right) \tag{2.3.25}$$

in the case of frequency modulation (2.3.2), and

$$D(\omega) \approx 8.5 \cdot 10^{-3} \frac{\epsilon^2 s^{4/3}}{\lambda^2 \Omega q} \exp\left(-2\pi\left(\frac{\omega}{\Delta\omega} - q\right)\right) \tag{2.3.26}$$

for the "random" perturbation.

Returning to the problem of modulation diffusion (Sec. 2.2) we can now give an explicit expression for its rate. Comparing (2.3.2) with (2.2.8), we find that $x = \theta_1 - m\nu t$. It then follows from (2.2.7) and (2.3.4) that $q = 1$ and $\omega = \omega_2 - m\nu$ for the first term in (2.2.7) and $\omega = \omega_2 + m\nu$ for the second term. If $\lambda\Omega \ll \nu$, then, since the rate of diffusion depends exponentially on ω (2.3.25), the second term in (2.2.7) can be neglected. Outside the plateau ($|\omega| > \lambda\Omega$) the diffusion rate in I_2 is:

$$D_{I_2} \approx \frac{\mu^2 a_1^2 a_2^2 \ln s}{8\lambda^2 \Omega} \cdot \exp\left\{-2\pi\left(\frac{|\omega_2 - m\nu|}{\lambda\Omega} - 1\right)\right\} \tag{2.3.27}$$

Besides external frequency modulation some "self-modulation" is possible and always present actually due to the phase oscillations of the unperturbed variables (including the unperturbed frequencies) under the action of a resonant perturbation. Since the frequency of phase oscillations $\Omega_\Phi \to 0$ near the separatrix of a nonlinear resonance, the corresponding modulation resonances do always overlap, forming a stochastic layer along the separatrix. The motion of the system

along this layer has been called Arnold diffusion, and was discussed in detail, for example, in [18]. We note that the rate dependence of the Arnold diffusion on the perturbation frequency:

$$D_A(\omega) \alpha e^{-\pi\omega/\Omega_\Phi}$$

is similar to expression (2.3.10) for modulation diffusion. This similarity becomes still more complete if we note that the halfwidth of the Fourier spectrum of the motion in the stochastic layer near the separatrix (the quantity analogous to $\Delta\omega$ for modulation diffusion) is equal to $2\Omega_\Phi$. It then follows, in particular, that the diffusion rates in both cases are comparable in magnitude (for $\Delta\omega \sim \Omega_\Phi$).

There are, however, two fundamental differences between the two processes:

1. Arnold diffusion is universal in the sense that it persists for arbitrarily weak perturbation, whereas modulational diffusion has a threshold, determined by the overlapping of resonances in the multiplet;

2. the width of the modulation stochastic layer generally greatly exceeds the width of the layer in which Arnold diffusion occurs.

Thus, if modulation stochastic layers are formed, diffusion along them is on the average much faster than Arnold diffusion.

3. *Transient Stochasticity in Quantum Dynamics.*

Despite the seeming paradox, one can now regard it as rigorously proven that the motion of certain simple, completely deterministic systems in classical mechanics leads to a (literally) random process. Moreover, one can apparently say that the very concept of randomness is now most naturally defined in terms of the stochastic motion of dynamical systems of classical mechanics as a certain limiting case of a deterministic process.

We also understand the mechanism giving rise to such an extremely complex and diverse process, associated with strong local instability of the motion. In particular, we may consider that such an instability as it gradually "discloses," in time, the intricacy and peculiarity of each particular realization of the random process that was already imposed in the exactly assigned initial conditions of the classical motion [33]. In this connection we should emphasize that the statistical properties of the classical motion are not related to the "practical indeterminacy of the initial conditions," as is often supposed, but even manifest themselves in the individual trajectory.

On the other hand, this same local instability itself leads to a strong dependence of the dynamical picture of the motion, not only on the initial conditions, but also on various slight perturbations of the system, including the various approximations both in each particular problem, as well as in the whole scheme of the classical mechanics. An important question arises: to what extent do all these approximations change the statistical properties of the classical dynamical system?

At first glance it may seem that this problem is solved by using the concept of *structural stability* of a dynamical system. Indeed, many stochastic systems, for example, all Anosov systems, are structurally stable, and consequently, even though individual trajectories of such systems are extremely sensitive to small perturbations, the overall structure of the motion and, in particular, its statistical properties change only insignificantly. However, the mathematical theory of structural stability of dynamical systems, despite its seeming generality, has its limitations even in the domain of classical mechanics (cf. Sec. 4.2 below). Still more unclear beforehand is the influence of quantum effects which, small in a sense, are of an extremely fundamental nature. In other words, the problem arises to study the quantum mechanical behavior of dynamical systems that are stochastic in the classical limit.

A great deal of work has already been devoted to this problem. The possible approaches here are of all sorts; roughly they can be divided into two main trends. In the first the authors start from the fundamental distinction between classical and quantum dynamics, associated with the discreteness of the energy (and frequency) spectrum of the quantum motion. We shall discuss this problem in Sec. 3.1. On these grounds some authors simply decline to consider the problem of quantum stochasticity [34]. Others take a more constructive position: accepting, explicitly or implicity, the above-mentioned fundamental distinction between classical and quantum dynamics, they put the question differently (cf., for example, [35–38, 51, 56]): what are the peculiarities of the quantum dynamics of those systems that are stochastic in the classical limit?

The authors of the second trend attempt, on the contrary, to generalize all the properties and concepts of classical stochasticity to quantum systems in obvious contradiction to the philosophy of the first trend (cf., for example, [39–42]). We should state, that there are serious physical arguments in favor of this second trend, based on the correspondence principle, according to which, for large quantum numbers, there should be some sort of transition to classical mechanics, including also the stochastic motion. These general arguments can be supplemented by invoking the well known Ehrenfest theorem, from which it follows that a sufficiently narrow quantum packet moves along a classical trajectory, including the case of a stochastic trajectory (cf. Sec. 3.3).

Apparently the first attempt at resolving the above contradiction was that of Krylov [43], who tried to generalize the complementarity principle to a relation between micro- and macro-descriptions of a quantum system. This interesting approach has as yet not been developed further. Below we shall consider another approach, based on the introduction of different time scales of the quantum motion.

3.1. *Almost-Periodicity of the Quantum Evolution.*

We shall begin our discussion with the problem of the discreteness of quantum spectra, which essentially limits the possible statistical properties of a quantum motion and, in particular, completely excludes stochasticity in the classical sense of the word (Sec. 2). Apparently Krylov [43] had been the first to call attention to this difficulty, and later on it was discussed also in other papers (cf., for example, [44, 45, 34]). Indeed, the discreteness of the spectrum implies an almost-periodic time evolution of both the wave function of the system and its density matrix (or Wigner function). In classical mechanics this type of motion is usually regarded as the opposite limit to the stochastic case, and as characteristic for a completely integrable system. We note that for convenience of comparison with quantum mechanics it is useful to go over from the usual picture of the motion of the individual classical system along a trajectory to the evolution of some function in the phase space of the system (for example, but not necessarily, the distribution function of an ensemble of systems) according to the Liouville equation. The spectrum of the latter can be either discrete (regular motion) or continuous (stochasticity).

In view of the importance of the spectral characteristics of the motion, we shall try to answer the question of how general the assertion about discreteness of a quantum spectrum really is. In so far as we are referring to the simplest quantum problems, described by the Schrödinger equations, discreteness of the spectrum is a rigorous mathematical result under the additional condition of bound-

edness of the system in phase space (including boundedness in energy, i.e., for closed systems). The spectrum of nonclosed systems where energy is not conserved may be continuous (cf. Sec. 3.2). We mention, however, that just as in classical mechanics, a nonclosed system is only a simplified model of some more complicated closed system. Therefore the pecularities of the dynamics of nonclosed systems are not of a principal importance.

A more important question is about the spectrum of other quantum equations, for example, those of quantum field theory and its existing or future generalizations, including nonlinear ones. May it not turn out that the Schrödinger equation, which only approximately describes the simplest quantum systems, is exceptional in this respect, and that some nonlinear generalization of the field equations has already led or will lead in the future to a continuous spectrum and classical stochasticity in quantum mechanics?

We should like to present here some simple physical arguments in favor of that the discreteness of the spectrum of a bounded quantum system is a fundamental feature of quantum mechanics. Our arguments are based on one of the basic statistical properties of classical dynamics, the so-called mixing. On the one hand this property directly leads to a diffusion of the system in phase space and, on the other, is related to the continuous spectrum of the motion, or of the Liouville operator. Perhaps we should mention here a delicate mathematical point: a continuous spectrum is equivalent to a somewhat weaker statistical property, that is called weak mixing. We shall, however, not enter into details here.

A continuous spectrum of the motion means that some aperiodic process is going on in the system, even though the motion itself is stationary. Such an aperiodic process is the irreversible relaxation of the distribution function to a steady-state one (a constant). If we expand the initial distribution function within a bounded region, for example, in Fourier series, the relaxation process means "disappearing" all Fourier components but the constant. But since both classical and quantum mechanics are reversible, this "disappearing" can only be explained in that the nonzero wave vectors of the Fourier components are growing indefinitely (aperiodically), i.e., are "disappearing" at infinity. In classical mechanics the wave vector of a distribution function is a purely kinematic quantity, and there are no restrictions in principle on its change. In contrast to this, in quantum mechanics the wave vector of the ψ function or of the

density matrix is related to the momentum, and consequently also to the energy of the system. Thus for a closed quantum system the aperiodic process described above is impossible, which results in a discrete spectrum of frequencies (and energies). This limitation seems to be fundamental and not related to any specific quantum equations. This last statement should be understood in the sense that, for the description of a quantum system only those equations, linear or nonlinear, are suitable that automatically guarantee discreteness of the quantum spectrum. Very likely all these (nonlinear) equations are completely integrable.

Thus it seems to us that one of the fundamental characteristics of quantum dynamics is the discreteness of quantum spectra and, consequently, almost-periodicity of the quantum evolution. But this means that, at least asymptotically in time ($t \to \infty$), the stochastic motion of a quantum system is actually impossible. The only statistical property, and the weakest one, that can be present in this limit of quantum motion is ergodicity (cf. [51, 56], and also Sec. 3.4). There are two basic problems associated with quantum ergodicity. The first is the investigation of the distribution of quantum levels [35, 36, 57], and the second is the ergodic properties of the eigenfunctions [51].

On the other hand, for a quantum system that is stochastic in the classical limit, a narrow wave packet does nevertheless move along the stochastic trajectory (Ehrenfest theorem)! True, as we know, the packets are spreading. But the rate of spreading can be made arbitrarily small if we go sufficiently far into the quasiclassical region. Thus, at least over a certain period of time, the quantum motion will be just as stochastic, in particular random, as the classical motion. This suggests the idea that to resolve the apparent contradiction between discreteness of the quantum spectrum and the correspondence principle one should introduce different time scales for the quantum motion. Actually we already know two such scales. One of them is $t \gtrsim T_d$ and may be called the *discrete scale*, over which there is fully manifested the discreteness of the spectrum that is characteristic for quantum systems. In the opposite limit $t \lesssim T_r$, which we shall call the *random scale*, the quantum motion is close to the classical limit, provided of course we impose the additional restriction on the quantum initial state whose wave function must be a narrow packet. As we shall see, only over this time scale can the quantum system be stochastic or random.

Now our main problem is to clarify the following question: do the

two limits T_r and T_d coincide (in order of magnitude) and, if not, what is the character of the motion between them? This problem was studied in [46] by numerical simulation of a simple quantum system, though, it is true, not in as clear a formulation as we can now give it. In the next section we give a brief description and analysis of the results of this work.

3.2. *A Simple Model of "Quantum Stochasticity."*

As the simplest model of a quantum system, in [46] the quantum analog of the standard mapping (2.1.1) was chosen. This model was selected for the following reasons. First, its dynamics in the classical limit had already been studied in detail [18]. Secondly, many particular problems in classical mechanics lead to the standard mapping. Finally, this model is a nonclosed system (the mapping is physically equivalent to a driving periodic perturbation), for which, in principle, a continuous spectrum is not excluded as it is for a closed system.

The model considered is a rotator in an external field with the Hamiltonian:

$$\hat{H} = -\frac{\hbar^2}{2}\frac{\partial^2}{\partial\theta^2} + \tilde{k}\cos\theta\delta_{\tilde{T}}(\tau) \tag{3.2.1}$$

where θ is the angle variable, $\tilde{k}$ a parameter characterizing the perturbation strength, $\delta_{\tilde{T}}(\tau) = \sum_{n=-\infty}^{\infty}\delta(\tau - n\tilde{T})$ is the periodic delta function.

The corresponding classical problem has the Hamiltonian:

$$H = \frac{p^2}{2} + \tilde{k}\cos\theta\delta_{\tilde{T}}(\tau) \tag{3.2.2}$$

and because of the periodicity of the perturbation the motion of the rotator can be described by the mapping:

$$\begin{aligned} \bar{p} &= p + \tilde{k}\sin\theta \\ \bar{\theta} &= \theta + \tilde{T}\bar{p} \end{aligned} \tag{3.2.3}$$

which reduces to the standard mapping with parameter $K = \tilde{k}\tilde{T}$.

We express the solution of the quantum problem in terms of the eigenfunctions of the free rotator:

$$\psi(\theta,\tau) = \sum_{n=-\infty}^{\infty} A_n(\tau)\frac{e^{in\theta}}{\sqrt{2\pi}} \tag{3.2.4}$$

in the form of a mapping for the amplitudes A_n over a period of the perturbation [46]:

$$\bar{A}_n = \sum_{m=-\infty}^{\infty} F_{nm}A_m \tag{3.2.5}$$

where

$$F_{nm} = (-i)^{n-m}\exp\left(-i\frac{Tm^2}{2}\right)J_{n-m}(k);$$

$J_l(k)$ is a Bessel function; $k = \tilde{k}/\hbar$; $T = \hbar\tilde{T}$. From the properties of Bessel functions it follows that one "kick" (iteration) couples (to exponential accuracy) approximately $2k$ levels, so the sum in (3.2.5) actually contains about $2k$ terms, a fact which was also used in the numerical simulation of the model (3.2.1).

The numerical experiments showed that the motion of the quantum system (3.2.1) has the following interesting feature. For $kT > 1$ and $k > 1$, in the quantum system, as in the classical case, there is diffusion in momentum p at a rate

$$D_p = \frac{\Delta\langle p^2\rangle}{\Delta t} = 2\frac{\Delta E}{\Delta t} \approx \frac{k^2}{2} \tag{3.2.6}$$

where

$$E = \sum_{n=-\infty}^{\infty}\frac{n^2}{2}|A_n|^2 \tag{3.2.7}$$

is the average energy of the rotator. Yet, the diffusion rate remains close to the classical value only over a certain time interval t^*. When $t > t^*$ the diffusion rate drops substantially (cf. Fig. 5), and the diffusion practically ceases at a very large time. We shall call this phenomenon the diffusion limitation. The time t^* increases with increasing k. Here t is integer and dimensionless time measured in the number of iterations.

When $t > t^*$ the distribution over the levels, in normalized coordinates $X = n^2/k^2t$, $f_N(n) = |A_n|^2\cdot\sqrt{\pi t}\,k$, is also rather different from the classical distribution: $f_N = e^{-X}$ (cf. Fig. 6). In computation we used various initial conditions: excitation only of the lowest level ($n_0 = 0$, uniform distribution in θ); excitation up to the hundred lowest levels with random amplitudes; a Gaussian distribution of width $10 \lesssim \Delta n \lesssim 200$ around the level $n_0 = 0, 500, 1000$ (the total number of levels in the model reached 4001). No significant dependence of the motion on initial conditions was observed.

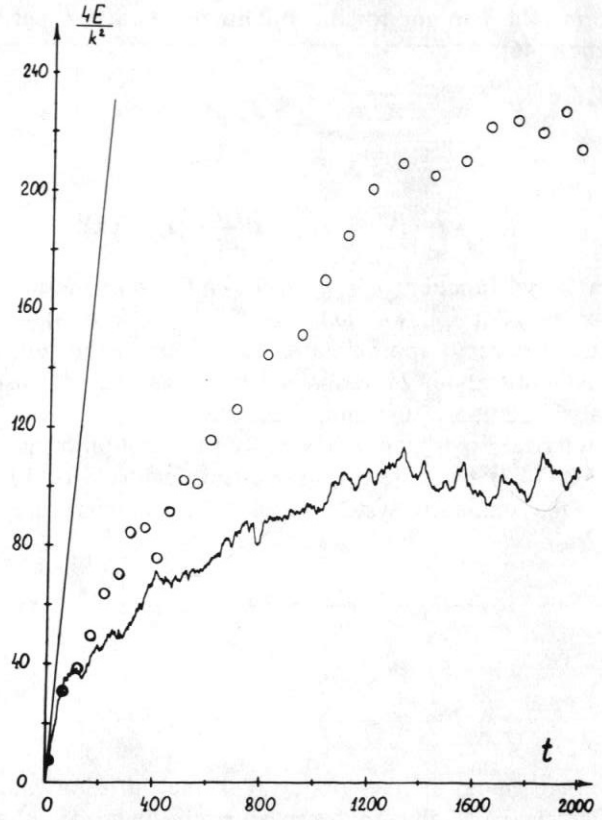

Figure 5. Dependence of rotator energy E on the time for the system (3.2.1) for $k = 20$; $T = 0.25$; $t = 2000$. The straight line corresponds to classical diffusion; ○— classical model of quantum stochasticity (4.1.1), the wiggly curve is the numerical result for (3.2.10).

Supplementary numerical experiments [47] showed that for a time $t < t^*$ the characteristics of the quantum motion were close to classical. Thus, we compared the dependence of the diffusion rate D_p on the parameter kT (for the classical system this question was studied in [18]). The results of this experiment showed a good agreement between these dependences in the classical and quantum cases: for the quantum problem we also observed oscillations of D_p in parameter kT and with the same period (cf. Fig. 7).

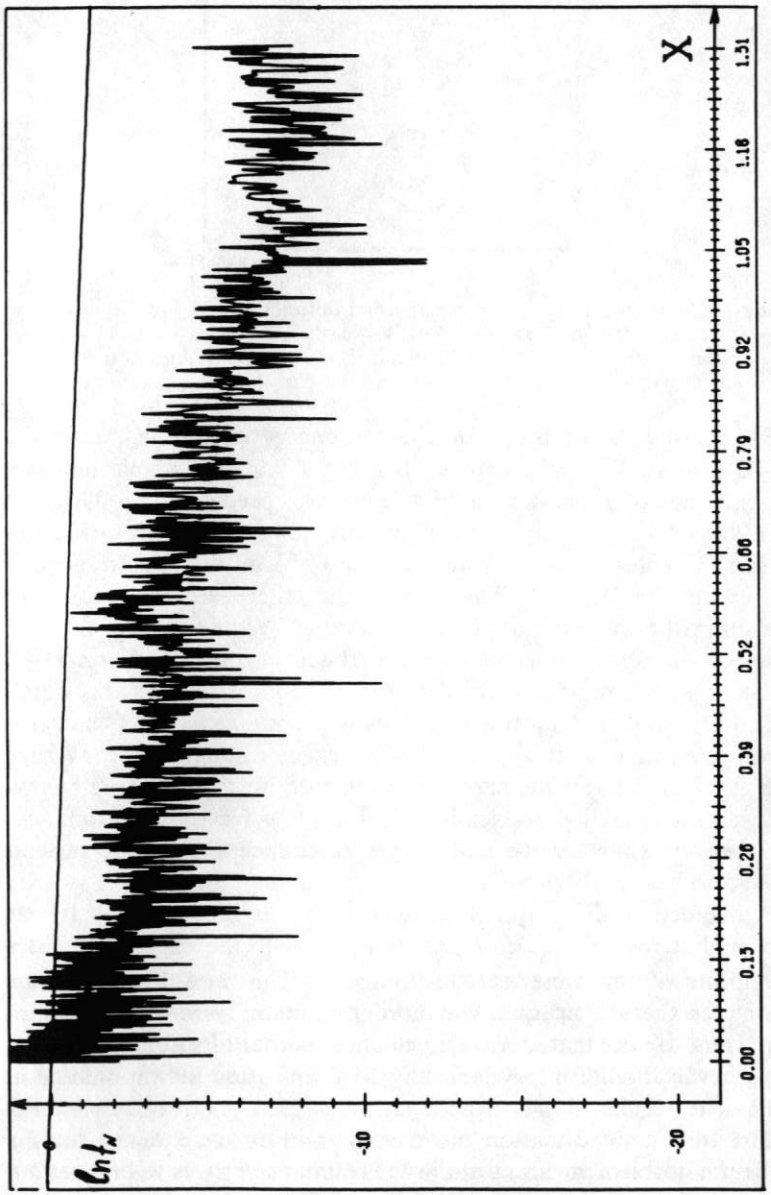

Figure 6. Distribution function over the unperturbed levels of the system (3.2.1) in normalized coordinates (cf. Sec. 3.2). The straight line corresponds to the classical distribution function; the wiggly line is the numerical result.

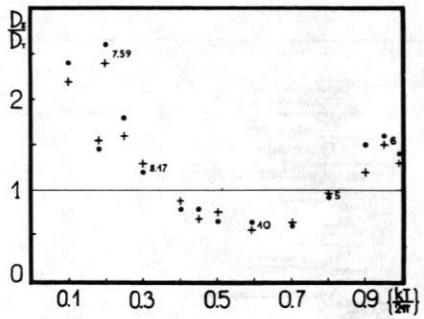

Figure 7. Dependence of ratio of experimental diffusion rate D_E to the theoretical $D_T = k^2/2$ on the fractional part $\{kT/2\pi\}$: •—for the classical system (3.2.2); +—for the quantum system (3.2.1) with $k \approx 40$. Numbers at some points are values of kT.

For $kT < 1$, $k > 1$ the change of the energy is bounded, as in the classical limit. The same is true when $k \lesssim 1$, $kT > 1$, which indicates the existence of a quantum stability border as predicted in [40]. In the case considered, the mechanism of this quantum stability is fairly understandable from (3.2.5). In fact, for $k \ll 1$ all the F_{nm} are negligible except for $F_{nm} \approx 1$. This means that there are practically no transitions between the unperturbed levels. We may assume that the quantum stability border corresponds roughly to the condition $k \sim 1$.

There is still another special type of motion of this system, which was discovered in [46] and called *quantum resonance*. It occurs for $T = 4\pi m$, where m is any integer. At exact resonance the average energy of the rotator increases proportionally to t^2. The same behavior was discovered numerically also for some fractional resonances $T = 4\pi p/q$, while for the half-integer resonance $T = 2\pi$ the motion proved to be strictly periodic.

A detailed study of quantum resonance was done in [48]. It was shown that for any integers p, q, but $p/q = \frac{1}{2}$, the energy increases asymptotically in time as t^2 for any k. This means that in the resonance there is no quantum border of stability ($k \sim 1$). It is also important to note that there is no classical border of stability ($kT \approx 1$) either, even though the system may be deep inside the quasiclassical region.

The full set of quantum resonances is everywhere dense (in T), while the quasienergy spectrum in the resonance proves to be continuous. At the same time, it was shown in [48] that for irrational values of T/π (whose measure is unity) the effect of the resonances is unimportant and that therefore the phenomenon of the diffusion limitation requires separate investigation.

The results of the investigations presented in this Section indicate an essential difference in the behavior of the quantum system as compared to classical at a sufficiently long time ($t > t^*$). Special numerical experiments showed that this time scale (t^*) is much greater than the time for spreading of packets, which under the experimental conditions was only one or two kicks. Thus the results of the numerical simulation indicate that the scales T_r and T_d introduced in Sec. 3.1 are very different ($T_r \ll T_d$), and that the motion when $t \lesssim T_d$ is characterized by classical diffusion. We shall still consider this problem further below. Indirect confirmation of the considerable difference between these scales is the absence of any indication as to the local instability of the quantum motion, according to the results of [46].

3.3. *Quasiclassical Approximation.*

The numerical experiments described in Sec. 3.2 showed that in the quasiclassical region ($k \gg 1$, $T \ll 1$, $kT = \text{const}$), when $kT > 1$ at least over a certain time interval some statistical characteristics of the quantum motion are close to classical. We shall show that this result can be obtained in the quasiclassical approximation. To do this we use the familiar quasiclassical representation for the wave function (cf., for example, [50]):

$$\psi(x,\tau) = \sum_{l=1}^{N} |\mathcal{J}_l|^{-1/2} \exp\left(iS_l(x)/\hbar - i\frac{\pi}{2}\mu_l\right) \times \varphi_0\left(x_0^l(x,\tau)\right) + O(k^{-1}) \tag{3.3.1}$$

The sum over l represents the leading term of the quasiclassical expansion, which as a rule is all that is considered by most authors. The sum goes over all classical trajectories that reach the point x at the time τ and satisfy the initial conditions

$$x_0(x,\tau) = x_0^l, \qquad p_0(x_0^l) = \left.\frac{\partial S_0(x_0)}{\partial x_0}\right|_{x_0 = x_0^l} \tag{3.3.2}$$

The initial wave function has the form

$$\psi(x_0,0) = \varphi_0(x_0)\exp\left(i\frac{S_0(x_0)}{\hbar}\right);$$

the Jacobian of the classical trajectory is $\mathcal{J}_l(x,\tau) = (\partial x(x_0,\tau)/\partial x_0)|_{x_0=x_0^l}$; $S_l(x,\tau)$ is the action along the classical trajectory joining the points x_0^l and x, while μ_l is the Morse index of the trajectory. The quantum corrections are represented in (3.3.1) by the term $O(k^{-1})$. They are usually small, although, as will be shown in Sec. 3.5, their magnitude increases with time and at a large time their contribution to (3.3.1) becomes substantial.

For stochastic systems, because of local instability of the trajectories, the number N of terms in the sum (3.3.1) and the Jacobian $\mathcal{J}_l(x,t) = (\partial x^l(x_0,\tau)/\partial x_0)$ increase exponentially with time: $N\sim \exp(h\tau)$, $\mathcal{J}_l \sim \exp(h\tau)$, where h is the KS-entropy.

Stochasticity of the classical system also leads to exponentially rapid spreading of the quasiclassical packet. For the example of the model (3.2.3) ($\hbar = 1$) we consider this question in more detail, since the spreading of the packet determines the time scale T_r, introduced in Sec. 3.1, over which the quantum motion can be completely random. To estimate this scale we note that the physical meaning of the leading term of the quasiclassical expansion (3.3.1) is simply that the initial quantum state $\varphi_0(x_0)$ propagates along the classical trajectories. Consequently the spreading of the quantum packet can be estimated roughly as the spreading of a beam of classical trajectories (in doing this we can neglect interference terms, as we shall show later in this Section). The rate of the packet spreading is determined by the classical KS-entropy h of the system, but the total time of spreading t_s depends on the initial dimensions of the packet: $\Delta\theta_0$ in phase and Δp_0 in momentum (the quantum number of the rotator). We assume that the packet has spread out completely when its final size $\Delta\theta \sim 1$ or when $\Delta p \sim 1/T = k/K$, $K = kT$ is the classical stability parameter for the system (3.2.3). The condition on Δp comes from the second equation in (3.2.3), since when $\Delta p \cdot T \gtrsim 1$ the size $\Delta\theta$ becomes $\gtrsim 1$ over one period of the perturbation. Taking into account that from the uncertainty relation, $\Delta\theta_0 \gtrsim 1/\Delta p_0$ while $\Delta p_0 \gtrsim 1$, we find the time for complete spreading of the packet in phase to be $t_s^{(\theta)} \lesssim \ln(\Delta p_0)/h$, and in momentum $t_s^{(p)} \lesssim \ln(k/K \cdot \Delta p_0)/h$. Actually the time for spreading of the packet will be of the order of the smaller of $t_s^{(\theta)}; t_s^{(p)}$. From the condition $t_s^{(\theta)} \sim t_s^{(p)}$, we find $\Delta p_0 \sim \sqrt{k/K}$, corresponding to the largest

$$t_s \sim \frac{\ln(k/K)}{2h} = \frac{|\ln T|}{2h} \qquad (3.3.3)$$

For typical values of the model parameters ($k = 40$; $K = 5$) the time $t_s \sim 1$ in agreement with the results of the numerical experiments (Sec. 3.2).

The scale (3.3.3) is generally very small and depends weakly on the parameter of the quasiclassical approximation k. Nevertheless, the condition for the applicability of (3.3.1) is the smallness of the further terms in the expansion (3.3.1) ($O(k^{-1})$), which leads to the time scale far in excess of t_s (cf. Sec. 3.5).

We see from (3.3.1) that the quasiclassical expansion is incorrect near degenerate stationary points, at which $\mathcal{J}_l(x) = 0$. The wave function has a caustic at such points. If there are q trajectories with caustics, then in the sum (3.3.1) there still remain $N - q$ quasiclassical terms (without singularities). The number q, like N, increases exponentially in time, but since the size of the caustic is finite and small ($\sim k^{-2/3}$, cf. [50]) and the caustics are distributed more or less uniformly in θ, the quantity $q \sim k^{-2/3} \cdot N \ll N$. We also note that the height of the peak of the ψ-function near a caustic decreases exponentially with time $\sim k^{1/6}\exp(-ht)$ as well as that of the quasiclassical terms. From this, in contrast to [38], we arrive at the conclusion that the effect of the caustics is at any time small and can be neglected. This result is confirmed by the numerical experiments carried out in [47].

Regarding the quantum corrections to the main quasiclassical term (3.3.1) as small, we find the time dependence of the rotator energy:

$$E(t) = \frac{1}{2}\int_0^{2\pi} \left| \frac{\partial \psi(x,t)}{\partial x} \right|^2 dx \qquad (3.3.4)$$

The main contribution comes from the differentiation of the action in the exponent. Differentiation of the coefficient and the phase shift μ_l give contributions that do not increase with time and are of order of k^{-1} as compared to the leading term:

$$E(t) = \frac{1}{2}\int_0^{2\pi} dx \left\{ \sum_{l,l_1=1}^{N} p_l(x) p_{l_1}(x) |\mathcal{J}_l \mathcal{J}_{l_1}|^{-1/2} \right.$$
$$\cdot \exp\left[i\left(S_l(x) - S_{l_1}(x) - \frac{\pi}{2}(\mu_l - \mu_{l_1}) \right) \right]$$
$$\left. \cdot \varphi_0\left(x_0^l(x,t)\right) \varphi_0\left(x_0^{l_1}(x,t)\right) \right\} \qquad (3.3.5)$$

where $p_l(x) = (\partial S_l(x)/\partial x)$ is the classical momentum along the lth trajectory leading to the point x; $x_0^l(x,t)$ is the initial point of this trajectory as a function of the final point x.

Let us examine the contribution from interference terms with $l \neq l_1$. They are $N_{\text{int}} \sim N^2$ in number, and the magnitude of each term is

$$R \sim \mathcal{J}^{-1} \int_0^{2\pi} dx \exp(i(S_l(x) - S_{l_1}(x))) \sim \exp(-2ht) \sim N^{-2}$$

The integral appearing in R is a typical correlation function, decaying exponentially in time because of the stochasticity of the classical motion. Thus we have a sum of N_{int} random quantities with amplitudes $R \sim N^{-2}$, which is equal to $\sum_{\text{int}} \sim \sqrt{N_{\text{int}}}\, R \sim N^{-1}$. This estimate is not applicable in the absence of stochasticity of the classical motion. However, the interference terms can also be neglected in this case. This follows from a universal estimate, valid both for stochastic and for regular motions in the classical limit [49]. Thus the interference terms with $l \neq l_1$ in (3.3.5) can be neglected, and there remains only the sum over $l = l_1$, giving the classical value of the energy.

Thus the leading term of the quasiclassical approximation (3.3.1) does not explain the observed diffusion limitation for the quantum system. The latter apparently is related to quantum corrections which, though small in the quasiclassical region, may nevertheless increase with time. This question will be considered in Sec. 3.5. As a preliminary, in the next section we shall obtain some simple estimates of quantum effects in the quasiclassical region.

3.4. *Graphic Picture of Transient Stochasticity.*

A possible explanation of the diffusion limitation described in Sec. 3.2 is that the quasienergy spectrum of this nonclosed system, which could in principle be continuous, is actually discrete. This hypothesis is confirmed to some extent by our direct numerical determination of the quasienergy spectrum in this model. The spectrum obtained clearly contains a strong discrete component, although, of course, the results do not permit us to guarantee the absence of any continuous component. Let us assume, however, that the spectrum is purely discrete with average spacing Δ between neighboring lines. From the uncertainty relation between frequency and time it follows that the discreteness of the spectrum will manifest itself only when $t \gtrsim 1/\Delta$, while for $t \lesssim 1/\Delta$ the spectrum can be regarded as quasicontinuous,

i.e., the time evolution of the quantum state will be the same as, or close to, that for a continuous spectrum (cf. [58]). But a continuous spectrum of the motion implies, in particular, mixing and diffusion. Thus we may try to identify in order of magnitude the discrete scale T_d, introduced in Sec. 3.1, with the diffusion time scale t^* for the quantum model (3.2.1):

$$T_d \sim t^* \sim 1/\Delta \tag{3.4.1}$$

Actually a similar idea vas already put forward in [46], but there the quantity Δ was related to the unperturbed energy spectrum of the rotator. Actually Δ characterizes the discreteness of the quasienergy spectrum which is built up in the system under the action of the perturbation.

Since all the levels of the quasienergy are located within a bounded interval (2π in our case), $1/\Delta \sim N_\psi$, where N_ψ is the effective number of eigenfunctions of the perturbed system that determine the evolution of the given initial state $\psi(\theta, 0)$. We point out that the total number of eigenfunctions, and consequently, also the total number of the quasienergy levels, is infinite (if we disregard the highly improbable infinite degeneracy of a level). However, each particular state of the system can be effectively represented by some finite number of eigenfunctions N_ψ.

An upper bound for N_ψ can be estimated as follows. According to the numerical data in Sec. 3.2 the diffusion drops sharply when $t > t^*$. Let us assume that the diffusion finally stops completely. This means that the perturbation acting on the free rotator couples a finite number of unperturbed states, namely the number of states that fall in the interval of the diffusion $\Delta p(t^*)$ over the time t^* (in order of magnitude). It is clear that this will also be the order of magnitude of the maximal number of eigenfunctions representing the state of the system within this interval Δp. Whence

$$N_\psi \sim \Delta p(t^*) \sim k\sqrt{t^*} \tag{3.4.2}$$

Substituting this estimate in (3.4.1), we obtain:

$$t^* \sim k^2 \sim D_p^{(cl)} \tag{3.4.3}$$

This estimate, apparently, does not contradict the numerical experiment, according to which the average value $\langle t^*/k^2 \rangle$ is ≈ 0.07 (cf. Sec. 3.6).

The last estimate in (3.4.3) emphasizes the connection of the statistical characteristics of the quantum motion (in this case the

diffusion scale t^*) with stochasticity in the classical limit, where the diffusion rate is $D_p^{(cl)} \approx k^2/2$.

Comparing the estimate for $t^* \sim T_d$ in (3.4.3) with that for the scale of spreading $t_s \sim T_r$ in (3.3.3), we see that in the quasiclassical region ($k \gg 1$) both scales actually have fairly different orders of magnitude, indeed ($T_r \ll T_d$) in agreement with the numerical results (Sec. 3.2). The question to what extent this conclusion is general for quantum dynamics of course remains open.

A more serious question concerns the role of initial conditions in this problem. Indeed, the very fact that the diffusion rate drops with time shows that this rate, in general, depends on the initial state of the system. On the other hand, among the several hundred initial states that were actually used in the numerical experiments there was none with an initial diffusion rate significantly less than the classical value. This shows that initial states with a reduced diffusion rate are extremely specific. One can reach the same conclusion in a different way. The estimate (3.4.2) gives the total number of states in the interval $\Delta p(t^*)$. The fact that the observed value of the diffusion scale t^* always corresponds more or less to this estimate shows that for a wide class of initial conditions most of the N_ψ eigenfunctions are actually excited. This means, in turn, that the eigenfunctions have a property resembling ergodicity: The projections of almost any ψ-vector on each of the eigenfunctions are close in magnitude. It is clear that this cannot be true for any quantum system. It is natural to associate this ergodicity of the eigenfunctions with the stochastic motion in the classical limit. This approach was apparently first used in [51] (cf. also [56]).

These same considerations enable us to understand the character and the peculiarities of the nondiffusing initial states in the stochastic region ($kT > 1$). It is clear that such states must be a superposition of a small number of eigenfunctions (in the limit, just one eigenfunction). It then also follows that such an initial state is a very special superposition of a large number ($\sim \Delta p(t^*) \sim k^2$) of states of the free rotator.

Our picture of the transient stochasticity may be checked by changing the quantum model. In particular, we may pose the question whether one could choose such a quantum (nonclosed) system to eliminate the diffusion limitation ($t^* \to \infty$). It turns out that this is possible indeed! In order to understand how one needs to change the original quantum model, we call attention to the following peculiarity of the mechanism of diffusion limitation. From a comparison of

(3.4.1) and (3.4.2) it is clear that the limitation occurs because the number of states in the diffusion interval $\Delta p(t) \sim k\sqrt{t}$ increases more slowly than the diffusion scale $T_d \sim t$. So one naturally gets the idea of making the perturbation parameter k variable, increasing with time in such a way that $\Delta p(t)$ would increase faster than t. It is true that then the perturbation of the rotator becomes aperiodic, and the concept of quasienergy strictly speaking loses its meaning. However, we may regard the model with variable $k(t)$ as a simplified version of a model with $k(n)$, depending on the level number of the free rotator which increases with time as the result of diffusion. Such a situation is apparently typical for quantum systems, and is related to the decrease in spacing between energy levels with increasing quantum numbers (cf. Secs. 3.5 and 3.6).

Suppose, for example,

$$k(t) = k_0 t^\alpha \tag{3.4.4}$$

where α is some constant. Then

$$\Delta p(t) \sim k_0 t^{\alpha + 1/2} \tag{3.4.5}$$

and we can make the assumption that when $\alpha \gtrsim \frac{1}{2}$ the diffusion continues unbounded. When $0 < \alpha < \frac{1}{2}$ the diffusion scale also increases. From (3.4.5) and (3.4.1) we find analogously to the above:

$$t^* \sim k_0^{1/(1/2-\alpha)} \tag{3.4.6}$$

The results of preliminary computational experiments with variable $k(t)$, described below in Sec. 3.6, do indicate such an effect, indeed.

Another more general and more rigorous method for estimating the diffusion scale T_d is to use the quasiclassical approximation to calculate the time evolution of the quantum state. Since the leading term of this approximation does not explain the observed diffusion limitation (Sec. 3.3) and, consequently, does not reflect the discreteness of the quantum system, it is obvious that the effect we are interested in is contained in the quantum corrections to the quasiclassical approximation, to whose estimate we now turn.

3.5. *Quantum Effects in the Quasiclassical Region.*

Using the results of Maslov [49, 50], we determine the time scale over which the quasiclassical approximation is applicable for quantum systems that are stochastic in the classical limit. A detailed treatment of this problem is given in [47].

Suppose that the classical system is described by the Hamiltonian $H = H_0(I) + \epsilon V(I,\theta,\tau)$, where I and θ are the action and phase of the unperturbed problem, $\epsilon \ll 1$. In this case it is sufficient for studying quantum corrections to take the expansion of H near the initial I_0 up to the terms $(\Delta I)^2$. When $I_0/\hbar \gg 1$ the standard quantization [40, 52] gives the Hamiltonian:

$$\hat{H} = \omega\hat{I} + \gamma\hat{I}^2 + \epsilon\Big[V(I_0,\theta,\tau) + \frac{1}{2}(\hat{I}V_1(\theta,\tau) + V_1(\theta,\tau)\hat{I}) + \frac{1}{2}\hat{I}V_2(\theta,\tau)\hat{I}\Big] \quad (3.5.1)$$

where

$$\omega = \frac{dH_0}{dI}\Big|_{I=I_0}, \qquad \gamma = \frac{1}{2}\frac{d\omega}{dI}\Big|_{I=I_0},$$
$$V_1 = \frac{dV}{dI}\Big|_{I=I_0}, \qquad V_2 = \frac{d^2V}{dI^2}\Big|_{I=I_0}, \qquad \hat{I} = -i\hbar\frac{\partial}{\partial\theta}.$$

Following [49, 50], we get the asymptotic quasiclassical expansion for the wave function satisfying the Schrödinger equation with the Hamiltonian (3.5.1) and the initial condition $\psi(\theta,\tau=0) = \varphi_0(\theta)\exp(iS_0(\theta)/\hbar)$:

$$\psi(\theta,\tau) = \sum_{l=1}^{N} |\mathcal{J}_l|^{-1/2}\exp\Big(\frac{i}{\hbar}S_l(\theta,\tau) - i\frac{\pi}{2}\mu_l\Big) \cdot \Big\{\sum_{m=0}^{\infty}\big[\hat{L}_l^m\varphi_0(\theta_0)\big]\Big|_{\theta_0=\theta_0^l(\theta,\tau)}\Big\} \quad (3.5.2)$$

where the summation in l goes over all classical trajectories arriving at the point θ at time τ and satisfying the initial conditions:

$$\theta_0(\theta,\tau) = \theta_0^l, \qquad I_0(\theta_0) = \frac{\partial s}{\partial\theta_0}\Big|_{\theta_0=\theta_0^l},$$
$$\mathcal{J}_l = \frac{\partial\theta(\theta_0,\tau)}{\partial\theta_0}\Big|_{\theta_0=\theta_0^l}$$

Here $S_l(\theta,\tau)$ is the action along the classical trajectory joining θ_0^l and θ; μ_l is the Morse index, while the operator $\hat{L}_l$ is defined by

$$\hat{L}_l\varphi_0(\theta_0) = i\hbar\int_0^\tau\Big\{\Big(\gamma + \frac{\epsilon}{2}V_2\Big)|\mathcal{J}_l|^{1/2}\Big(\mathcal{J}_l^{-1}\frac{\partial}{\partial\theta_0}\Big)^2\cdot(|\mathcal{J}_l|^{-1/2}\varphi_0) + \frac{\epsilon}{2}|\mathcal{J}_l|^{-3/2}\frac{\partial V_2}{\partial\theta_0}(|\mathcal{J}_l|^{-1/2}\varphi_0)\Big\}d\tau \quad (3.5.3)$$

The sum over m in (3.5.2) is actually an expansion in powers of $\hbar$. The main quantum correction comes from the term with $m = 1$, i.e., from the expression (3.5.3). To the accuracy of terms that do not increase with time, it is sufficient, in calculating the quantum correction to differentiate only the Jacobian $\mathcal{J}_l(\theta_0)$. We define the quantum correction $\delta_1^{(l)}$ by the equation: $\hat{L}_l\varphi_0 \approx \delta_1^{(l)}\varphi_0$. Then from (3.5.3) we find

$$|\delta_1^{(l)}| = \Big|i\hbar\int_0^\tau\Big\{\Big(\gamma + \frac{\epsilon}{2}V_2\Big)\Big[\frac{5}{4}\mathcal{J}_l^{-4}\Big(\frac{\partial\mathcal{J}_l}{\partial\theta_0}\Big)^2 - \frac{1}{2}\mathcal{J}_l^{-3}\frac{\partial^2\mathcal{J}_l}{\partial\theta_0^2}\Big] - \frac{\epsilon}{4}\mathcal{J}_l^{-3}\frac{\partial V_2}{\partial\theta_0}\frac{\partial\mathcal{J}_l}{\partial\theta_0}\Big\}d\tau\Big| \ll 1 \quad (3.5.4)$$

The last inequality is the condition for applicability of the quasiclassical approximation. The integral over time in (3.5.4) should be understood as the difference of the primitives at the time τ and 0. Since at an intermediate time $\mathcal{J}_l$ may vanish (at crossing a caustic), the result of the integration is not sign-definite. Since $\mathcal{J}_l \sim \exp(h\tau)$, $(\partial\mathcal{J}_l/\partial\theta_0) \sim \exp(2h\tau)$, $(\partial^2\mathcal{J}_l/\partial\theta_0^2) \sim \exp(3h\tau)$, the correction δ_1 increases no faster than τ, and thus the quasiclassical approximation is applicable over the time scale $t_0 \propto 1/\hbar$.

Now let us consider a special form of the perturbation: $\epsilon V(I,\theta)\cdot g(\tau)$, where $g(\tau)$ has the form of kicks which act over a time T_0, and follow each other in an interval T ($T \gg T_0$). Suppose that the change of the action by a kick is ΔI and that the criterion for stochasticity $K \approx \gamma T\Delta I \gg 1$ [18, 41, 53] is satisfied. Splitting the integral in (3.5.4) into a sum of integrals over the intervals $T + T_0$, and assuming the terms in the sum to be statistically independent because of the stochasticity of the classical system, while

$$\mathcal{J}(Tt + T_0 + \tau) \sim \mathcal{J}(Tt + T_0)\cdot\Big(1 + K\frac{\tau}{T}\Big);$$
$$\frac{\partial^n\mathcal{J}}{\partial\theta_0^n} \sim \mathcal{J}^{n+1}(Tt + T_0)\cdot\Big(1 + K\frac{\tau}{T}\Big),$$

we find that $\delta_1^{(l)}$ increases on the average according to the law

$$\langle|\delta_1^{(l)}|^2\rangle \sim \hbar^2\sum_{j=0}^{t}\Big(\frac{1}{\overline{\Delta I}_l(j)} + \gamma^{(l)}T_0\Big)^2 \quad (3.5.5)$$

where $\overline{\Delta I}_l(j) = \langle(\Delta I_l(j))^2\rangle^{1/2}$ is the change in the action by a kick, averaged over the random phase θ. Since $\Delta I \sim \epsilon$, the terms ϵV_2 in (3.5.4) can be neglected.

Let us calculate, as an example, the quantum correction for the

system (3.2.1), using (3.5.4). According to (3.2.2) and (3.2.3) we get the expression for $p(\tau), \theta(\tau)$ within the interval between successive kicks ($\hbar = 1$):

$$\begin{aligned} p(\tau) &= p_t + k \sin\theta_t \\ \theta(\tau) &= \theta_t + p_t\tau + k\tau \sin\theta_t \end{aligned} \tag{3.5.6}$$

where p_t, θ_t are the values of the variables immediately before the last kick. From (3.2.3) we get the relation:

$$\frac{\partial\theta_t}{\partial\theta_0} = (kT)^{t-1}\cos\theta_{t-1}\cos\theta_{t-2}\ldots\cos\theta_0 + 0(1/kT)$$

according to which we have

$$\frac{\partial\theta(\tau)}{\partial\theta_0} = \frac{\partial\theta_t}{\partial\theta_0}(1 + k\tau\cos\theta_t) + 0(1/kT)$$

$$\frac{\partial^2\theta(\tau)}{\partial\theta_0^2} = -\left(\frac{\partial\theta_t}{\partial\theta_0}\right)^2 K\tau\sin\theta_t + 0(1/kT)$$

$$\frac{\partial^3\theta(\tau)}{\partial\theta_0^3} = -\left(\frac{\partial\theta_t}{\partial\theta_0}\right)^3 k\tau\cos\theta_t + 0(1/kT)$$

Splitting up the integral in (3.5.4) into a sum of integrals from t to $t+1$, we get:

$$\delta_1^{(l)} = \frac{i}{2}\sum_{j=0}^{t}\int_0^T\left\{\frac{5}{4}\frac{(k\tau)^2\sin^2\theta_j^l}{\left(1 + k\tau\cos\theta_j^l\right)^2} + \frac{1}{2}\cdot\frac{k\tau\cos\theta_j^l}{\left(1 + k\tau\cos\theta_j^l\right)^3}\right\}d\tau + O(1/kT)$$

After integrating we find the expression for $\delta_1^{(l)}$:

$$\delta_1^{(l)} = \frac{i}{8}\sum_{j=0}^{t}\frac{3\cos^2\theta_j^l + 5\sin^2\theta_i^l}{k\cos^3\theta_j^l} \tag{3.5.7}$$

Because of the stochasticity of the classical trajectory, the sum over j increases as $t^{1/2}$ and, consequently, on the average

$$\delta_1 \sim it^{1/2}/k \tag{3.5.8}$$

Thus, for a time

$$t \lesssim t_0 \sim k^2 \tag{3.5.9}$$

the quantum corrections are small and the characteristics of the quantum system agree with the classical ones to the accuracy of $O(k^{-1})$.

For $t \sim t_0$ the correction $\delta_1 \sim 1$ (the higher corrections in $\hbar$ are also ~ 1) and the quasiclassical approximation becomes completely inapplicable. Thus it is natural to expect that for $t \gtrsim t_0$ the characteristics of the quantum problem, for example, the energy of the rotator, will deviate significantly from their classical values. Consequently, we can give an estimate for the time t^*, after which the diffusion limitation begins as was observed in [46]:

$$t^* \sim t_0 \sim k^2 \tag{3.5.10}$$

This estimate agrees with the estimate (3.4.3) obtained above by a different method.

We note that in the system (3.2.1) the parameters of the quasiclassical approximation k, T do not depend on the level number n, and hence the diffusion upward over the levels does not improve the quasiclassical approximation. Yet, in many systems this approximation does improve with increasing n (cf. below). We may therefore expect that with sufficiently rapid diffusion the quantum corrections in such systems will grow much more slowly than in (3.2.1).

As an example we consider a system with the Hamiltonian (3.2.1), in which k has a power dependence on the time: $k(t) = k_0 t^\alpha$ (cf. Sec. 3.4). As a rule k is an increasing function of the action $k = k(I)$, and consequently of the time since under stochasticity I grows with time. The latter is just represented in the model chosen which is also useful for numerical study. Nevertheless we must note that in systems with $k = k(I)$ the situation turns out to be more complicated (cf. Sec. 3.6) and that therefore this model should be regarded only as a crude example.

When $k_0 T > 1$ the variable θ after a few kicks already becomes random, and the average change in p per kick is

$$\langle|\Delta p(t)|^2\rangle = k_0^2 t^{2\alpha}\langle\sin^2\theta(t)\rangle = \frac{k_0^2 t^{2\alpha}}{2}$$

Whence, the diffusion law in energy ($\langle\Delta p\rangle = 0$) is:

$$E(t) \approx \frac{k_0^2}{4(1+2\alpha)}t^{1+2\alpha} + E(0) \tag{3.5.11}$$

The expression for δ_1 is obtained in the same way as for (3.5.7), but now with $k = k(j)$. On the average $|\delta_1|^2$ increases as

$$\langle|\delta_1|^2\rangle \sim \sum_{j=0}^{t} \frac{1}{k^2(j)} \approx \frac{t^{1-2\alpha}}{k_0^2(1-2\alpha)} \tag{3.5.12}$$

It follows from (3.5.12) that when $\alpha > \frac{1}{2}$ the corrections are always small, and the dependence of the energy on time is described by (3.5.11) for any time, which also agrees with the conclusion drawn in Sec. 3.4. The value $\alpha = \frac{1}{2}$ is a boundary one. In this case the diffusion scale $t_0 \sim \exp(k_0^2)$. When $0 \leqslant \alpha < \frac{1}{2}$ the quasiclassical approximation is valid for

$$t < t_0 \sim \left[k_0^2(1-2\alpha)\right]^{1/(1-2\alpha)} \tag{3.5.13}$$

and during this time the energy grows according to the classical law. This last estimate differs from the estimate (3.4.6) by a factor $(1-2\alpha)$, which, however, is important only for $\alpha \approx \frac{1}{2}$.

One can show that the relations $(\partial \bar{I}/\partial\theta_0) \sim \bar{I}^2$; $(\partial^n \bar{I}/\partial\theta_0^n) \sim \bar{I}^{n+1}$ do hold also for a continuous classical system. Then the integral in (3.2.4) can be split into a sum of integrals over time intervals $\Delta\tau \sim 1/\hbar$, which are statistically independent, and thus we find

$$|\delta_1^{(I)}|^2 \sim \hbar^2 \int_0^{\tau} \left(\gamma^{(I)}/h\right)^2 h\, dt \ll 1 \tag{3.5.14}$$

For $\gamma = \text{const}$, (3.5.14) gives $\delta_1 \sim (\hbar\gamma/h)(h\tau)^{1/2}$. Thus, for example, if $H = \gamma(I^2/2) + k\sum_{m=-M}^{m} \cos(\theta + m\Omega t + \varphi_m)$, where φ_m is a set of random phases and $M \gg s = (k\gamma)^{1/2}/\Omega \gg 1$, then $h \sim \Omega s^{4/3}$ [31] (cf. also Sec. 2.3) and the diffusion scale $\tau_0 \sim h/\hbar^2\gamma^2$.

Thus, we managed to find out the conditions for applicability of the quasiclassical approximation (3.3.1) to a broad class of systems. At the same time the problem of the peculiarities of quantum dynamics for a larger time requires further investigations.

3.6. *Other Models.*

To check the theoretical predictions made in Secs. 3.4 and 3.5, we carried out a series of additional numerical experiments [47] for the rotator model (3.2.1) with $k = \text{const}$ and $k(t) = k_0 t^{\alpha}$ as well as for the model of a nonlinear oscillator under a driving perturbation, which was studied theoretically in [41].

From the numerical data, we determined the time t^* during which the diffusion is close to classical. We took for the value of t^* the moment in time starting from which the energy of the quantum rotator differed by 25% from the energy in the classical limit.

To check the functional dependence (3.5.13), we calculated the quantity

$$\delta = \left[\frac{(t^*)^{1-2\alpha}}{k_0^2(1-2\alpha)}\right]^{1/2}$$

The experimental results for the average value $\langle\delta\rangle$, the root-mean-square deviation σ_δ and the ranges of the parameters are given in Table 1. These results show that, in accordance with the theoretical predictions, the time t^* increases sharply with increasing both k and α. Unfortunately a more precise check of the functional dependence (3.5.13) could not be made because of the limited number of levels of the model and due to the sharp increase in computation time with the growth of k and α. We were able to observe clearly the diffusion limitation only for $\alpha < 0.35$ (cf. Figs. 8 and 9). It is important to note that, when $\alpha \geqslant 0.35$, not only does the diffusion law agree with the classical one, but the distribution function over system levels is close to the classical Gaussian distribution.

Now let us consider a nonlinear oscillator acted upon by a driving perturbation, described by the Hamiltonian:

$$\hat{H} = \omega_0\hat{n} + \gamma\hat{n}^2 + \tilde{g}_0(\hat{a}^+ + \hat{a})\delta_{\tilde{T}}(\tau) \tag{3.6.1}$$

where $\hat{n} = \hat{a}^+\hat{a}$; $\hat{a}^+$ and $\hat{a}$ are the creation and annihilation operators, with the commutator $[\hat{a}, \hat{a}^+] = \hbar$; γ is the nonlinearity; $\tilde{g}_0$ is a perturbation parameter. When $[\hat{a}, \hat{a}^+] = 0$, Eq. (3.6.1) describes a classical oscillator, while a^+ and a become classical canonical variables, whose dynamics can be given by the mapping:

$$\bar{a} = e^{-i\omega\tilde{T}}a - \tilde{g}_0 \tag{3.6.2}$$

where $\omega = \omega_0 + 2\gamma I$; $I = |a|^2$, $a = \sqrt{I}\, e^{i\theta}$. The criterion for stochasticity

Table 1

kT	k	α	t^*	δ	$\langle\delta\rangle$	$\sigma_\delta/\langle\delta\rangle$
5–36	5–80	0	5–320	0.14–0.50	0.27	0.32
5–10	5–10	0.1–0.35	40–500	0.53–1.7	1.1	0.31

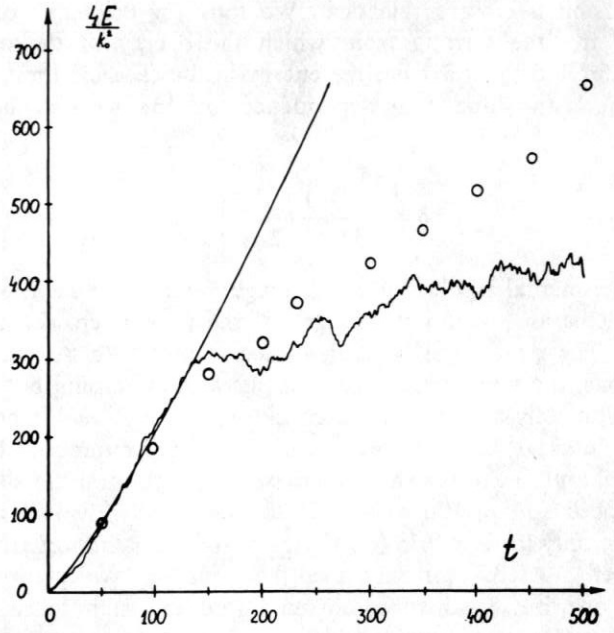

Figure 8. Dependence of rotator energy E on time for the system (3.2.1) for $k(t) = k_0 t^{\alpha}$; $\alpha = 0.1$; $k_0 = 5$; $T = 1$; $t = 500$. The solid curve corresponds to the classical diffusion (3.5.11); the wiggly curve is the numerical result; ○—the classical model of quantum stochasticity (4.1.1).

has the form:

$$K = 2\gamma \tilde{T} \tilde{g}_0 \sqrt{I_0} \gg 1 \tag{3.6.3}$$

and then [41]:

$$\begin{aligned} I(t) &= I_0 + \tilde{g}_0^2 t \\ (I - I_0)^2 &= 2\tilde{g}_0^2 I_0 t + 2\tilde{g}_0^4 t^2 \end{aligned} \tag{3.6.4}$$

In the case of quantum system (3.6.1) it is convenient to describe its dynamics in terms of the amplitude A_n of the unperturbed states (cf. Sec. 3.2):

$$i\dot{A}_n = (\omega_0 n + \hbar\gamma n^2)A_n + g_0\left(\sqrt{n+1}\, A_{n+1} + \sqrt{n}\, A_{n-1}\right)\delta_{\tilde{T}}(\tau) \tag{3.6.5}$$

where $g_0 = \tilde{g}_0/\hbar$ and $n = I/\hbar$ is the level number in the unperturbed system.

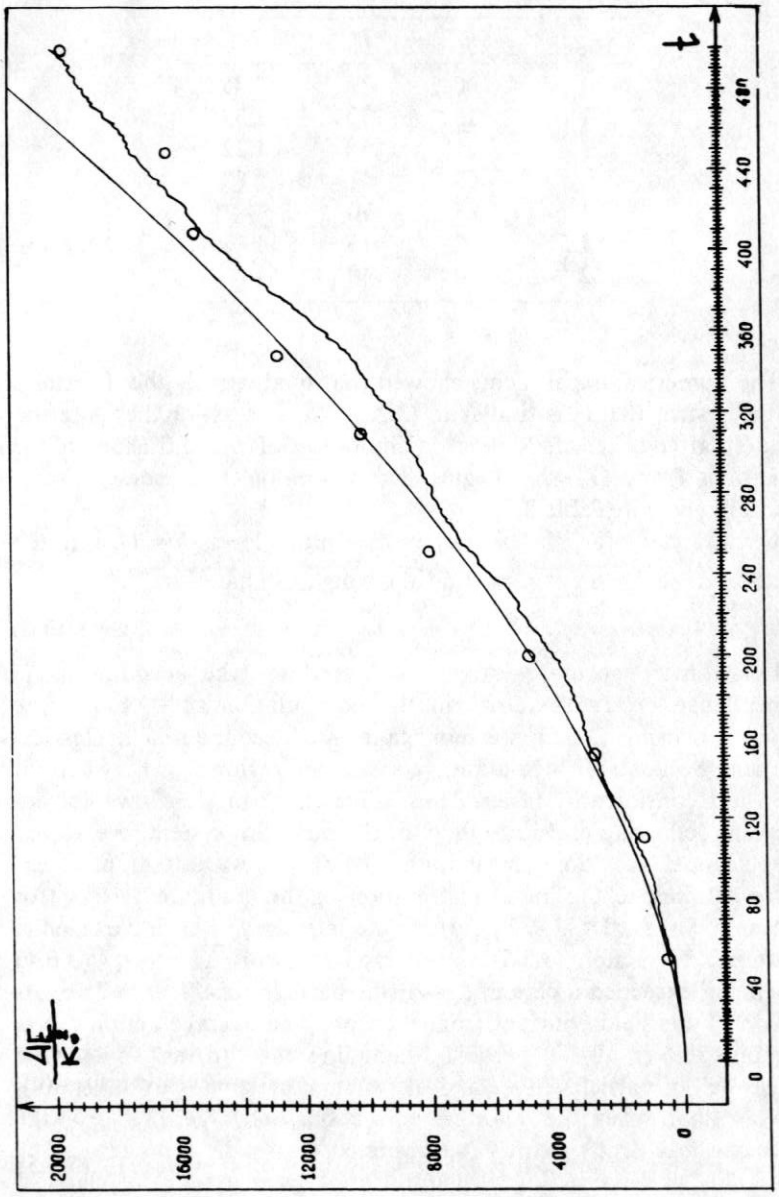

Figure 9. Same as Fig. 8, for $\alpha = 0.35$; $k_0 = 5$; $T = 1$; $t = 500$.

Table 2. $\omega_0 T = 1000$; $\gamma T = 1$

g_0	n_0	t^*	δ_{cr}
1	0	29	2.45
1	15	30	1.32
1	31	55	1.22
1	63	51	.87
1	83	70	—
1.5	0	15	1.12
2	0	40	1.

The numerical experiments showed that qualitatively the dynamics of the system (3.6.1) is similar to (3.2.1). As well as for the quantum rotator, after a certain time t^* a limitation of the diffusion in the quantities I and $(I - I_0)^2$ begins. The values of t^* for some parameters are given in Table 2.

Using (3.5.5) for $g_0^2 \ll n_0$ (n_0 is the initial level, $\hbar = 1$) and the relation $\Delta I \approx 2g_0\sqrt{I}\cos\theta$, we find the rough estimate for t^*:

$$t^* \sim g_0^2 n_0 \tag{3.6.6}$$

For a more accurate estimate we need to take account of ΔI dependence on I. Therefore in the computation of δ_1 along the trajectory, using (3.5.5), we must take into account that a classical particle, because of fluctuation, gets into the region $I < I_0$, where δ_1 increases considerably faster. Thus, for a check of (3.5.5) we considered the following classical model of the quantum system. We solved the classical equations of motion (3.6.2) for $N_0 \approx 1000$ particles, corresponding to the initial distribution of the quantum system (for example, $I = I_0$, $0 \leqslant \theta \leqslant 2\pi$). Along the trajectory of each particle the quantum correction (3.5.5) was computed (with $\overline{\Delta I} = g_0 I_l^{1/2}$), and when $\delta_1^{(l)}$ exceeded a certain $\delta_{cr} \sim 1$, the particle was "frozen," i.e., its action I_l was held constant from then on. The average action I was computed over all N_0 particles, including the "frozen" ones. The "freezing" of particles in a classical system corresponds to the empirical fact that, when the quantum corrections are large, ($\delta_1^{(l)} \gtrsim 1$) the diffusion rate drops sharply (we assumed that it drops to zero). The possibility of representing a quantum motion as a beam of classical trajectories arises from the smallness of the interference terms when $|\delta_1^{(l)}| \lesssim 1$ (cf. Sec. 3.3).

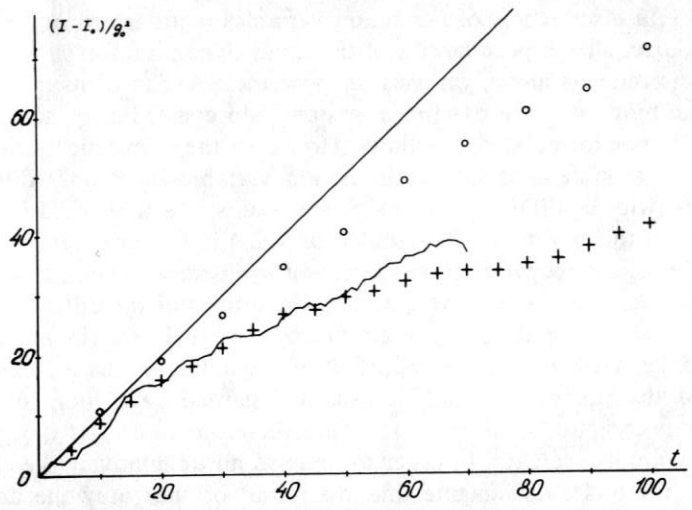

Figure 10. Dependence of action of a nonlinear oscillator on time for the system (3.6.1) with $n_0 = 15$; $g_0 = 1$; $\omega_0 T = 1000$; $\gamma T = 1$. The straight line corresponds to classical diffusion (3.6.4), the wiggly line is the numerical result; +—the "frozen particle" model; ○—the classical model of quantum stochasticity (4.1.2).

The critical value δ_{cr} was determined from the condition that the action I, calculated on the "frozen particle" model, be close to its quantum value. It turned out that, by varying this only parameter (cf. Table 2) over a small interval, one can achieve a good agreement between the quantum characteristics and those of the "frozen particle" model (cf. Fig. 10) for a wide range of the parameters n_0, g_0 (cf. Table 2). This shows the validity of the estimate (3.5.5) and, also, that by using the proposed classical model one can describe the quantum dynamics of the system (3.6.1) over a time far in excess of t^*.

4. *Discreteness of Dynamical Space and Quantum Effects.*

In the preceding sections we have found that, except for some special cases, in a quantum system there can occur only transient, or temporary stochasticity of the motion, which has a natural explanation on the basis of the discreteness of the quantum spectrum. One may, however, approach this problem in a different way, and call attention to a still more fundamental and also well known peculiarity of quantum dynamics, namely the discreteness of the quantum phase space. Particularly, in terms of action-angle variables this manifests

itself in a discreteness of the action variables (with arbitrary phases). Of course, all the peculiarities of quantum dynamics don't reduce to this discreteness alone, yet we may pose the question of its influence on the motion of the dynamical system. More specifically, the question may be formulated as follows: How does the stochastic motion of a classical system change if the action variables take only discrete values (with continuous phases)? Some results of a numerical investigation of this question are presented in Sec. 4.1. To our great surprise, the simple discretization of the action of a classical dynamical system reproduces qualitatively the quantum limitations of the diffusion!

At first glance this does seem strange, since in the language of computer mathematics discretization of the action is just a rounding off of that quantity, which is usually regarded as a more or less random computational error. It would therefore seem that the diffusion can only increase. In order to understand qualitatively the effect of diffusion, let us imagine that we round off not only the action variables, but also the phases, i.e., all the dynamical variables. Then instead of the continuous classical trajectory we would get a sequence of transitions on the finite lattice of rounded-off values. Whatever the law for these transitions, sooner or later we get onto one of the previously occupied nodes of the lattice, and then, because of the deterministic nature of the system, all the succeeding points will repeat exactly. But this means that *all* trajectories of *any* dynamical system on a finite lattice are periodic, which of course completely excludes any diffusion as $t \to \infty$. And now we recall that in numerical simulation of a dynamical system on a digital computer we always have just this situation—a finite number lattice instead of the continuous dynamical space of the simulated system. It then follows, in particular, that numerical simulation can give only transient stochasticity. Taking account of the large and ever increasing role of numerical experiments in the investigation of various dynamical systems, we meet a serious problem: to what extent is such simulation adequate for real physical systems? This problem is discussed in Sec. 4.2.

4.1. *Classical Model of "Quantum Stochasticity".*

In this Section we shall present and discuss some results of numerical simulation concerning the impact of discreteness of the phase space on classical dynamics. As the simplest model of such a "discrete

dynamics" we choose the mapping:

$$\bar{p} = p + [k \sin x] \qquad \bar{x} = x + T\bar{p} \tag{4.1.1}$$

where the square brackets denote taking the integer part. Without that operation the system (4.1.1) would be equivalent to the standard mapping with the parameter $K = kT$, whose properties were described in Secs. 2.1 and 3.2. Taking the integer part in (4.1.1) lends to this system some resemblance to the quantum standard mapping, namely the action p then runs only over integer values ($\hbar = 1$), while the parameter k in (4.1.1), just as for the quantum system (Sec. 3.2), characterizes the maximal number of "quanta" given to the system by one "kick" of the driving perturbation. We note that the system (4.1.1) also has a stability border $|k| < 1$ (cf. Sec. 3.2), if the integer part for negative numbers is taken by the rule: $[y] = -[|y|]$ $(y < 0)$.

In Fig. 5 the circles show the time dependence of the energy of the system (4.1.1) averaged over 400 trajectories with various initial conditions (p_0, x_0), where the distribution over phases x_0 was taken to be uniform. One clearly sees a significant difference from the continuous classical model. As a result one can draw the interesting conclusion that the discreteness, introduced for the momentum p, leads to a significant limitation of diffusion, although the quantum dynamics proves to be somewhat more stable than "discrete" dynamics. A similar result was also obtained for the time dependent $k = k_0 t^{\alpha}$ (cf. Secs. 3.6 and Figs. 8, 9).

For comparison we also considered the classical discrete model of a quantum nonlinear oscillator, whose motion is described by the mapping (3.6.2). Discreteness was introduced as in the previous case by taking the integer part of the change in the action as the result of a kick:

$$\bar{I} = I + [\Delta I] = I + [(a + a^{+})g_0 + g_0^2] \tag{4.1.2}$$

Then, from the integer value of $\bar{I}$, we recalculated the quantities a, a^{+}, and computed the rotation which leaves the action unchanged.

The results of the numerical experiments on this discrete model showed in this case also (cf. Fig. 10) a noticeable limitation of the diffusion compared to the classical model. It should be emphasized that this property appears to be common to all discrete models, and does not depend, in particular, on the choice of the initial distribution

(p_0, x_0) for the packet of trajectories. Thus, for example, instead of a uniform distribution in phase x_0, we assigned a random distribution over the same interval $(0 \leqslant x_0 \leqslant 2\pi)$. But the results remained about the same (to within fluctuations). Similarly, the result did not depend on the number N_0 of trajectories over which we determined the average energy, so long as N_0 was chosen sufficiently large $(N_0 \gtrsim 300)$.

4.2. *Numerical Simulation of Dynamical Stochasticity.*

In the preceding Section 4.1 it was shown that a simple discretization of the action variable of a classical dynamical system reproduces qualitatively the quantum effect of the diffusion limitation of this system in the stochastic region. In our opinion, this result is of importance in two ways. In quantum mechanics it opens the possibility of imitating certain quantum effects by means of "classical" models, where analysis of the motion as well as numerical simulation are much simpler. On the other hand, the above result poses a very serious question concerning the adequacy of numerical simulation of classical stochasticity. We proceed to a brief discussion of these questions.

To be specific, we shall consider a two-dimensional mapping, for example, the standard mapping (2.1.1) or its equivalent (3.2.3). Suppose that the number of the mantissa digits in the computer is m. Then on a unit interval any quantity can have $M = 2^m$ different values, and a region of phase space with area s in this example consists of sM^2 points. The maximum period of motion over this region is obviously $T_{\max} = sM^2$ iterations of the mapping. But for a "random walk" over the lattice the average period of motion is much less: $\langle T \rangle \sim M\sqrt{s}$, since with increasing time of the motion along the trajectory, there is an increasing probability of coming back to one of its earlier points.* In analogy to the arguments in Sec. 3.4 we can conclude that the quantity $\langle T \rangle$ also determines the largest time scale over which the spectrum of the motion can still be considered continuous, and over which, consequently, the diffusion still goes on. As in quantum dynamics, it is natural to call the regime of motion when $t \gtrsim \langle T \rangle$ the *discrete* regime. Here the discreteness of the phase space of the dynamical system manifests itself to the full, and the

*Our estimate for $\langle T \rangle$ differs from the result of [54], since it was assumed in that work that the discrete mapping was one-to-one, which generally is not the case.

motion is periodic. The boundary of this interval for the two-dimensional mapping can be written as

$$T_d \sim M\sqrt{S} \tag{4.2.1}$$

For a typical computer this scale is quite large ($M \sim 10^{15}$) and can be easily increased by many orders of magnitude if we go to double precision. Thus the discrete regime does not generally present a serious threat to numerical simulation. The exception may be those special cases where for some reason s is very small, i.e., the motion actually proceeds within a very small portion of the phase plane. This could happen, for example, if over some region the diffusion rate were quite small (cf. Sec. 2.1). In this case the actual area occupied by the trajectory is $s \sim |\Delta p| \sim \sqrt{Dt}$, where t is the time of motion. Then: $\langle T \rangle \sim M\sqrt{s} \sim t^{1/4} \cdot M \cdot D^{1/4} \gtrsim t$. The last inequality is the condition for the diffusion regime of motion. The restriction on the time of motion now takes the form $t < M^{4/3}D^{1/3}$. If the region with low diffusion rate has a size $\sim \Delta p_0 \ll 1$, the condition for crossing it can be written as:

$$D \gtrsim \frac{(\Delta p_0)^{3/2}}{M} \tag{4.2.2}$$

The diffusion limitation because of transition into the discrete regime of motion was apparently observed in some numerical experiments [55, 23] (cf. also Sec. 2.1).

The influence of discreteness of dynamical variables ("roundoff errors") is a characteristic example of a very small perturbation that nevertheless completely changes the dynamics of the system after a sufficiently long time, even if the system is structurally stable, say an Anosov system. The reason why the general theorem on structural stability is not applicable here is related to the singularity of the perturbation.

For the classical model of quantum stochasticity (4.1.1) similar estimates can be made as follows. Since the "quantum" of momentum is equal to 1, the number of different values of p over the time t is simply equal to the diffusional change $|\Delta p| \sim k\sqrt{t}$ (cf. Sec. 3.4). Although the phase x can have any value, it also changes in "quanta" $\sim p$. Hence, the number of different values of x over this same time can be estimated very roughly as $|\Delta x|/|p| \sim t$, where $|\Delta x| \sim |p|t$ is the diffusional change in x during the time t. Then the scale of discrete-

ness is $T_d \sim \sqrt{|\Delta p| \cdot t} \sim \sqrt{k}\, t^{3/4} \gtrsim t$. The last inequality just determines the order of magnitude of the time within which the diffusion occurs in the model (4.1.1): $t \lesssim k^2$, which agrees with the estimates for the quantum systems in Secs. 3.4 and 3.5. One can similarly also obtain estimates for varying $k(t)$.

A continuous spectrum and diffusion are important statistical properties of a dynamical system. Therefore the diffusion regime (when $t \lesssim T_d$) of quantum dynamics and of numerical simulation may be regarded as a particular (special) case of stochastic motion. This is the more justified that in this regime not only an average diffusion but also fluctuations of the diffusion distributed according to Gauss' law take place (cf., for example, [18,46] and Fig. 6), the latter being a much more delicate statistical property. In probability theory this property is the content of the central limit theorem. Yet, this is still not all. An even stronger statistical property is the so-called Bernouilli property related to the exponential instability of close trajectories. It is just such an instability that causes the dynamical system to behave like a random one.

In numerical simulation, the time scale t_s over which there occurs an exponential divergence of close trajectories is restricted by the minimal initial separation between trajectories $\sim M^{-1}$, whence

$$t_s \sim \frac{\ln M}{h} \sim m \tag{4.2.3}$$

where h is the entropy of the dynamical system. For a typical (good) computer the number of digits is $m \sim 100$ and cannot be significantly increased. Thus the scale t_s is inadmissibly short. In this connection the important question arises—which statistical properties are lost in numerical simulation over a time $t \gg t_s$?

There is no question that simulation over such an interval is not completely adequate for a continuous system. For example, we can follow a local instability only for $t \lesssim t_s$. In calculating the KS-entropy this difficulty can be avoided by the standard trick of averaging over many short segments of different trajectories. But this is not the same thing from the point of view of statistical properties of the motion.

For example, one of the simple consequences of the Bernouilli property of a dynamical system is the completeness of its symbolic trajectories (cf. Sec. 1). Even if we take the minimal partition of the phase space into just two cells, the total number of symbolic trajectories over the time (number of iterations) t would be $N_R = 2^t$. But the maximum number of different initial conditions is $N_c \sim M^2$, so that

they can provide the completeness only over an interval $t_R \sim \ln M \sim m$. This scale is of the same order at t_s (4.2.3) and, in analogy with quantum dynamics, it can be taken as the scale of randomness of the motion:

$$T_r \sim m \tag{4.2.4}$$

Although for $t \gg T_r$ the total number of trajectories in the computer is much less than the total number of symbolic trajectories for the simulated system, it is still so large ($\sim M^2 \sim 10^{30}$!), that an obvious incompleteness of the simulation is nearly unobservable. In this connection the question posed above may be reformulated as follows: do we really lose anything in simulation of stochasticity over the whole diffusion interval ($t \lesssim T_d$)?

Similar questions also arise in quantum dynamics, since the scale of randomness T_r, which can be identified with the scale of packet spreading t_s (3.3.3), proves to be also relatively short:

$$T_r \sim \frac{\ln(k)}{h} \tag{4.2.5}$$

where k is the parameter of the quasiclassical approximation.

References

1. F . Izrailev, Nearly Linear Mappings and their Applications, Physics D, 1980, in print.
2. D. D. Ryutov, G. V. Stupakov, JETP Lett. *26*, 186 (1977).
3. B. V. Chirikov, Plasma Physics *45*, 27 (1978); *58*, 80 (1979).
4. V. D. Il'in, A. N. Il'ina, JETP *72*, 983 (1977).
5. A. K. Nekrasov, Nucl. Fusion *10*, 387 (1970); E. F. Jaeger, A. J. Lichtenberg, M. A. Lieberman, Plasma Physics *14*, 1073 (1972).
6. G. M. Zaslavsky, B. V. Chfrikov, Usp. Fiz. Nauk *105*, 3 (1971).
7. V. M. Alekseev, M. V. Yakobson, Symbolic Dynamics and Hyperbolic Dynamical Systems, suppl. to the book of R. Bowen, Methods of Symbolic Dynamics, Mir, Moscow, 1979.
8. A. K. Zvonkin, L. A. Levin, Usp. Mat. Nauk *25*, 85 (1970).
9. Ya. G. Sinai, Usp. Mat. Nauk *25*, 141 (1970); Ya. B. Pesin Ya. G. Sinai, this volume, p.77 .
10. E. N. Lorenz, J. Atmosph. Sci. *20*, 130 (1963).
11. D. V. Anosov, Geodesic Flows on Closed Riemannian Manifolds with Negative Curvature, Repts. Steklov Math. Inst. *90*, 1967.
12. S. Smale, Bull. Amer. Math. Soc. *73*, 747 (1967).
13. B. V. Chirikov, F. M. Izrailev, Some Numerical Experiments with a Nonlinear Mapping: Stochastic Component. Coll. Int. CNRS #229, Transformations Ponctuelles et Leurs Applications (Toulouse 10–14 Sept. 1973), CNRS Paris (1976), p. 409; Degeneration of Turbulence in Simple Systems, Phys. Rep., 1980, in print.

14. M. I. Rabinovich, Usp. Fiz. Nauk *125*, 123 (1978); A. S. Pikovsky, M. I. Rabinovich, this volume, p. 165.
15. L. A. Bunimovich, Dokl. Akad Nauk SSSR *211*, 1024 (1973); Ya. B. Pesin, Usp. Mat. Nauk *32*, 55 (1977); L. A. Bunimovich, Comm. Math. Phys. *65*, 295 (1979).
16. N. N. Bogolyubov, Some Statistical Methods in Mathematical Physics, Ukr. SSR, 1945.
17. J. Ford, A Picture Book of Stochasticity, AIP Conference Proc., #46, 1978, p. 121.
18. B. V. Chirikov, Phys. Rep. *52*, 265 (1979).
19. V. I. Arnold, A. Avez, Ergodic Problems of Classical Mechanics (Benjamin, New York, 1968).
20. J. M. Greene, J. Math. Phys. *20*, 1183 (1979).
21. G. Schmidt, Stochasticity and Fixed Point Transitions, Centre de Phys. Theor. Ecole Polytech., 1980 (unpublished).
22. B. V. Chirikov, Nonlinear Resonance, Novosibirsk, Nov. St. Univ., 1977.
23. B. V. Chirikov, Interaction of Nonlinear Resonances, Novosibirsk, Nov. St. Univ., 1978.
24. D. F. Escande, F. Doveil, Renormalization Method for Computing a Stochasticity Threshold, Int. Conf. on Plasma Physics, Nagoya, 1980.
25. M. Aizenman, S. Goldstein, J. L. Lebowitz, Comm. Math. Phys., *39*, 289 (1975).
26. G. V. Gadiyak, F. M. Izrailev, B. V. Chirikov, Numerical Experiments on Universal Instability in Nonlinear Oscillator Systems (Arnold Diffusion), Repts. 7th Int. Conf. on Nonlinear Oscillations (Berlin, 1975), Akad. Verlag, Berlin, Vol. II, 1, p. 315.
27. B. V. Chirikov, J. Ford, F. Vivaldi, Some Numerical Studies of Arnold Diffusion in a Simple Model, in *Nonlinear Dynamics and the Beam-Beam Interaction*, AIP Conf. Proc. #57, 1979, p. 323.
28. B. V. Chirikov, Adiabatic Invariants and Stochasticity in Magnetic Confinement Systems, Int. Conf. on Plasma Physics, Nagoya, 1980.
29. J. L. Tennyson, M. A. Lieberman, A. J. Lichtenberg, Diffusion in Near-Integrable Hamiltonian Systems with Three Degrees of Freedom, in *Nonlinear Dynamics and the Beam-Beam Interaction*, AIP Conf. Proc. #57, 1979, p. 272.
30. C. Froeschle, Astrophys. and Space Sci. *14*, 110 (1971).
31. B. V. Chirikov, Investigations of the Theory of Nonlinear Resonance and Stochasticity, prepr. 267, Inst. Nucl. Phys. Siberian Sec. Acad. Sci. USSR, Novosibirsk, 1969 (CERN Transl. 71-40, Geneva, 1971).
32. A. B. Rochester, M. N. Rosenbluth, R. B. White, Phys. Rev. Lett. *42*, 1247 (1979).
33. B. V. Chirikov, Wiss. Zs. Humboldt-Univ. zu Berlin, Ges.-Sprachw. *24*, 215 (1975); B. V. Chirikov, The Nature of Statistical Laws in Classical Mechanics, prepr. Inst. Nucl. Phys. 78-66, Novosibirsk, 1978.
34. J. L. Lebowitz, O. Penrose, Physics Today, Feb. 1973, p. 23.
35. F. J. Dyson, J. Math. Phys. *3*, 140 (1962).
36. G. M. Zaslavsky, Usp. Fiz. Nauk *129*, 211 (1979).
37. I. C. Percival, Regular and Irregular Spectra in Molecules, Lecture Notes in Physics *93*, Springer, 1979, p. 259.
38. M. V. Berry et al., Ann. Phys. *122*, 26 (1979).
39. N. M. Pukhov, D. S. Chernavsky, Teor. Mat. Fiz. *7*, 219 (1971).
40. E. V. Shuryak, JETP *71*, 2039 (1976).
41. G. P. Berman, G. M. Zaslavsky, Physica *91A*, 450 (1978); *97A*, 367 (1979).
42. M. D. Srinivas, J. Math. Phys. *19*, 1952 (1978).
43. N. S. Krylov, Foundations of Statistical Mechanics, Princeton, 1979.
44. P. Bocchieri, A. Loinger, Phys. Rev. *107*, 337 (1957).
45. I. C. Percival, J. Math. Phys. *9*, 235 (1961).

46. G. Casati, B. V. Chirikov, J. Ford and F. M. Izrailev, Lecture Notes in Physics, v. 93, ed. G. Casati and J. Ford, Springer, New York, 1979, p. 334.
47. D. L. Shepelyansky, Quasiclassical Approximation for Stochastic Quantum Systems, prepr. Inst. Nucl. Phys. Siber. Sec. Acad. Sci. USSR 80-132, Novosibirsk, 1980.
48. F. M. Izrailev, D. L. Shepelyansky, Dokl. Akad. Nauk SSSR *249*, 1103 (1979): Teor. Mat. Fiz. *43*, 417 (1980).
49. V. P. Maslov, Zh. Vych. Mat. i Mat. Fiz. *1*, 638 (1961).
50. V. P. Maslov, M. V. Fedoryuk, Quasiclassical Approximation for the Equations of Quantum Mechanics. "Nauka," Moscow, 1976.
51. A. I. Shnirelman, Usp. Mat. Nauk *29*, 181 (1974).
52. V. V. Sokolov, Nonlinear Resonance of a Quantum Oscillator, prepr. Inst. Nucl. Phys. Siber. Sec. Acad Sci USSR, 78-50, 1978.
53. G. M. Zaslavsky, Statistical Irreversibility in Nonlinear Systems, "Nauka," Moscow, 1970.
54. F. Rannou, Astron. & Astroph. *31*, 289 (1974).
55. B. V. Chirikov, E. Keil, A. M. Sessler, J. Statist. Phys. *3*, 307 (1971).
56. K. S. J. Nordholm, S. A. Rice, J. Chem. Phys. *61*, 203 (1974).
57. M. V. Berry, Ann. Phys. April, 1980.
58. P. Brumer, M. Shapiro, Chem. Phys. Lett. *72*, 528 (1980).